UNIVERSIDAD CARLOS III DE MADRID working papers

UC3M Working papers
Economics
18-10
September, 2018
ISSN 2340-5031

Departamento de Economía
Universidad Carlos III de Madrid
Calle Madrid, 126
28903 Getafe (Spain)
Fax (34) 916249875

Seasonal Quasi-Vector Autoregressive Models with an Application to Crude Oil Production and Economic Activity in the United States and Canada

Szabolcs Blazsek
School of Business, Universidad Francisco Marroquín, Guatemala City 01010, Guatemala
Álvaro Escribano*
Department of Economics, Universidad Carlos III de Madrid, Getafe (Madrid) 28903, Spain
and
Adrian Licht
School of Business, Universidad Francisco Marroquín, Guatemala City 01010, Guatemala

Abstract

We introduce the Seasonal-QVAR (quasi-vector autoregressive) model that we apply to study the relationship between oil production and economic activity. Seasonal-QVAR is a score-driven nonlinear model for the multivariate t distribution. It is an alternative to the basic structural model that disentangles local level and stochastic seasonality. Seasonal-QVAR is robust to extreme observations and it is an extension of Seasonal-VARMA (VAR moving average). We use monthly data from world crude oil production growth, global real economic activity growth and the industrial production growths of the United States and Canada. We address an important economic question about the influence of world crude oil production on the industrial productions of the United States and Canada. We find that the effects of industrial production growth of the United States on world crude oil production growth are about six times higher for the basic structural model and Seasonal-VARMA than for Seasonal-QVAR. We also find that the effects of world crude oil production growth on the industrial production growth of Canada are positive for Seasonal-QVAR, but those effects are negative for Seasonal-VARMA. Likelihood-based performance metrics and transitivity arguments support the estimates of Seasonal-QVAR, as opposed to the basic structural model and Seasonal-VARMA.

KEY WORDS: Dynamic conditional score (DCS); Score-driven stochastic seasonality; Nonlinear multivariate dynamic location models; Basic structural model; Vector autoregressive moving average (VARMA) model.

Compiled: September 12, 2018

* Corresponding author. Department of Economics, Universidad Carlos III de Madrid, Calle Madrid 126, Getafe (Madrid) 28903, Spain. E-mail: alvaroe@eco.uc3m.es.

1. Introduction

In the present work, we introduce the new Seasonal-QVAR (quasi-vector autoregressive) model that includes nonlinear score-driven multivariate local level and stochastic seasonality components, and we apply this model to study the relationship between oil production and economic activity for the United States and Canada. An important property of Seasonal-QVAR, as opposed to multivariate time series models with Gaussian error terms, is that the QVAR filter is robust to extreme values in the noise. In this paper, we extend the results of Blazsek, Escribano, and Licht (2017) to Seasonal-QVAR, by deriving the (i) nonlinear infinite vector moving average VMA(∞) representation of the local level component, (ii) impulse response function (IRF), and (iii) conditions of consistency and asymptotic normality of the maximum likelihood (ML) estimator that include the condition of invertibility.

Seasonal-QVAR is a dynamic conditional score (DCS) model (Creal, Koopman, and Lucas 2013; Harvey 2013), in which the conditional score of the log-likelihood (LL) (hereinafter, score function) updates the vector of dependent variables and the noise term has a multivariate t distribution. DCS models are observation-driven time series models (Cox 1981). An example of those models is the Beta-t-GARCH (generalized autoregressive conditional heteroscedasticity) model (Harvey and Chakravarty 2008), which is an extension of the GARCH model (Engle 1982; Bollerslev 1986). Another example is the QAR model (Harvey 2013), which is an extension of the AR moving average (ARMA) model (Box and Jenkins 1970). With respect to the recent DCS models, we refer to the works of Blazsek and Escribano (2016) and Ayala, Blazsek, and Escribano (2017). Blazsek and Escribano (2016) suggest a DCS count panel data model, which is an alternative to the dynamic count panel data models of Blundell, Griffith, and Windmeijer (2002) and Wooldridge (2005). Ayala, Blazsek, and Escribano (2017) suggest DCS-EGARCH (exponential GARCH) models with score-driven shape parameters, which are extensions of the DCS-EGARCH models with constant shape parameters (see, for example, Harvey 2013).

Seasonal-QVAR is an alternative to the Gaussian multivariate Unobserved Components Model (UCM) with local level and stochastic seasonality (hereinafter, basic structural model)

(Harvey 1989), which is a widely-used model for macroeconomic and financial time series variables. Seasonal-QVAR is an extension of QVAR (Harvey 2013, Chapter 7; Blazsek, Escribano, and Licht 2017), that is also named as the dynamic conditional score model for the multivariate t distribution (Harvey 2013). Motivated by the recent applications of score-driven seasonality models to univariate time series (i.e., Harvey 2013; Harvey and Luati 2014; Caivano, Harvey, and Luati 2016; Ayala and Blazsek 2017, 2018; Blazsek and Hernández 2017), we extend QVAR by adding a multivariate score-driven seasonality component. Our paper is also related to the body of literature on VAR and VARMA models (see, for example, Sims 1980, 1986; Sims, Goldfeld, and Sachs 1982; Bernanke 1986; Blanchard and Watson 1986; Tiao and Tsay 1989; Stock and Watson 2001), because Seasonal-QVAR is a nonlinear extension of Gaussian Seasonal-VARMA.

We apply Seasonal-QVAR to a classic macroeconomic dataset: monthly data from the world crude oil production growth and global real economic activity growth variables for the period of March 1973 to December 2007. Both variables have significant seasonality components (Ye, Zyren, and Shore 2006 and Raunglerdpanyagul 1985, respectively), and the dataset includes several extreme observations (e.g., related to the 1973 and 1979 oil crises). The use of these variables is motivated by several works that study the question of how changes in supply and demand in the world crude oil market are related to economic growth (Blanchard 2002; Barsky and Kilian 2002, 2004; Hamilton 2003; Kilian 2008, 2009; Baumeister and Hamilton 2017).

We also apply Seasonal-QVAR to an extended macroeconomic datatset and address the important applied economic question about the influence of world crude oil production on the industrial productions of the United States and Canada. We study that question by using Seasonal-QVAR in a way that prior Gaussian multivariate models cannot. We use monthly data from world crude oil production growth and total industrial production growths of the United States and Canada for the period of March 1973 to February 2018. Our analysis is motivated by the following points: (i) the United States and Canada have important trade relations; (ii) those countries are among the largest crude oil producers in the world; (iii) current renegotiation of the North American Free Trade Agreement (NAFTA); (iv) we extend of the sample period of

previous studies on crude oil and industrial production (e.g., Nordhaus, Houthakker, and Sachs 1980; Kilian 2008; Peersman and Van Robays 2009; Baumeister and Peersman 2013).

To our knowledge, it is popular among practitioners to apply the following two-step estimation procedure to macroeconomic variables that involve seasonality components: Deseasonalize the macroeconomic time series in a first step, and undertake an IRF analysis in a second step for the deseasonalized time series. That approach assumes that the seasonal and non-seasonal shocks are uncorrelated, which may fail in practice. The two-step estimation procedure is not effective for Seasonal-QVAR, because both the local level component and the stochastic seasonality component are updated by the same score function term. In Seasonal-QVAR, the seasonal and non-seasonal shocks are correlated, motivating the joint estimation of multivariate local level and stochastic seasonality. In the present paper, we suggest an alternative approach to the recent UCM specification of Hindrayanto, Jacobs, Osborn, and Tian (2018).

The new nonlinear multivariate QVAR model is able to identify the seasonality that is hidden for the linear VARMA model. Seasonality is identified by the IRF estimates of QVAR, thus, QVAR can be applied in the detection of nonlinearities in time series data. Seasonal-QVAR effectively disentangles the local level and the stochastic seasonality components, as seasonality effects do not appear in the IRF estimates of Seasonal-QVAR. We show that Seasonal-QVAR is robust to extreme values in the noise, and the conditions of the consistency and asymptotic normality of the ML estimator are satisfied. The model diagnostic tests support the specification of Seasonal-QVAR, and we find that the likelihood-based performance of Seasonal-QVAR is superior to that of the basic structural model and Gaussian Seasonal-VARMA. These results can provide practitioners with a suggestion on the application of the nonlinear Seasonal-QVAR model to measure dynamic interaction effects among macroeconomic variables that involve seasonality, as an alternative to the application of the classic multivariate linear time series models.

The remainder of this paper is organized as follows. Section 2 presents the econometric models. Section 3 describes the empirical results for the classic macroeconomic data. Section 4 describes the empirical results for the extended macroeconomic data. Section 5 concludes.

2. Econometric models

2.1. Seasonal-QVAR

For y_t $(K \times 1)$ with $t = 1, \ldots, T$, the Seasonal-QVAR model is $y_t = c + \mu_t + s_t + v_t$, where c $(K \times 1)$ includes constant parameters, μ_t $(K \times 1)$ is the dynamic local level component, s_t $(K \times 1)$ is the dynamic seasonality component, and v_t $(K \times 1)$ is the reduced-form error term. The components μ_t and s_t are observable, conditional on the past information $(y_1, \ldots, y_{t-1})$.

We formulate the reduced-form error term v_t as multivariate i.i.d. $v_t \sim t_K(0, \Sigma_v, \nu)$, where $\Sigma_v = \Omega_v^{-1}(\Omega_v^{-1})'$ is positive definite and $\nu > 2$ is the degrees of freedom parameter (hence, the variance of v_t is finite). As a consequence, $E(v_t) = 0$ and $\text{Var}(v_t) = \Sigma_v \times \nu/(\nu - 2)$. We also introduce the multivariate i.i.d. structural-form error term $\epsilon_t = [\nu/(\nu-2)]^{-1/2}\Omega_v \times v_t$, for which $E(\epsilon_t) = 0$ and $\text{Var}(\epsilon_t) = I_K$. The log of the conditional density of y_t is

$$\ln f(y_t|y_1, \ldots, y_{t-1}) = \ln \Gamma\left(\frac{\nu + K}{2}\right) - \ln \Gamma\left(\frac{\nu}{2}\right) - \frac{K}{2}\ln(\pi\nu) \tag{1}$$

$$-\frac{1}{2}\ln|\Sigma_v| - \frac{\nu + K}{2}\ln\left(1 + \frac{v_t'\Sigma_v^{-1}v_t}{\nu}\right)$$

and the score function with respect to μ_t is

$$\frac{\partial \ln f(y_t|y_1, \ldots, y_{t-1})}{\partial \mu_t} = \frac{\nu + K}{\nu}\Sigma_v^{-1} \times \left(1 + \frac{v_t'\Sigma_v^{-1}v_t}{\nu}\right)^{-1} v_t = \frac{\nu + K}{\nu}\Sigma_v^{-1} \times u_t, \tag{2}$$

where u_t $(K \times 1)$ is the scaled score function vector; Harvey (2013, p. 211) shows that u_t is multivariate i.i.d. with zero mean and finite variance. In the definition of the score function, v_t is multiplied by the term $[1 + (v_t'\Sigma_v^{-1}v_t)/\nu]^{-1} = \nu/(\nu + v_t'\Sigma_v^{-1}v_t) \in (0, 1)$. As a consequence, the score function is always bounded by the reduced-form error term: $|u_t| < |v_t|$.

We formulate the local level component as $\mu_t = \Phi\mu_{t-1} + \Psi u_{t-1}$, where Φ $(K \times K)$ and Ψ $(K \times K)$ are time-constant parameter matrices, and μ_t is updated by the first lag of the scaled score function u_{t-1}. We initialize μ_t by using the unconditional mean $\mu_1 = E(\mu_1) = 0_{K\times 1}$. Alternatives to this initialization may also be used. For example, the elements of μ_1 may be

estimated as additional parameters in the joint estimation of all parameters of Seasonal-QVAR. We use $\mu_1 = 0_{K\times 1}$, in order to reduce the number of estimated parameters.

We formulate each element of the seasonality component $s_t = (s_{1,t}, \ldots, s_{K,t})'$ according to $s_{k,t} = D_t'\rho_{k,t}$ for each $k = 1, \ldots, K$, where $D_t = (D_{1,t}, \ldots, D_{S,t})'$ is a vector of seasonal dummy variables and $\rho_{k,t} = (\rho_{k,1,t}, \ldots, \rho_{k,S,t})'$ is a vector of dynamic seasonality parameters (S denotes the known period of the seasonality). Variable $\rho_{k,t}$ is updated according to the $I(1)$ equation $\rho_{k,t} = \rho_{k,t-1} + \gamma_{k,t}u_{k,t-1}$, where $\gamma_{k,t} = (\gamma_{k,1,t}, \ldots, \gamma_{k,S,t})'$ is a dynamic scaling parameter and $u_{k,t-1}$ is the k-th element of u_{t-1}. From Equation (1) we have $\partial \ln f(y_t|y_1, \ldots, y_{t-1})/\partial \mu_t = \partial \ln f(y_t|y_1, \ldots, y_{t-1})/\partial s_t$ hence the same updating term u_{t-1} is used for μ_t and s_t, which motivates the joint estimation of μ_t and s_t. Furthermore, each element of $\gamma_{k,t}$ is given by $\gamma_{k,j,t} = \gamma_{k,j}$ for $D_{j,t} = 1$ and $\gamma_{k,j,t} = -\gamma_{k,j}/(S-1)$ for $D_{j,t} = 0$, where $\gamma_{k,j}$ with $j = 1, \ldots, S$ are seasonality parameters to be estimated. This parameterization ensures that $\sum_{j=1}^{S} \gamma_{k,j,t} = 0$. As a consequence, $s_{k,t}$ is centered at zero for each dependent variable (we demonstrate this in the Appendix). The variable $s_{k,t}$ is a high-pass filter that compensates the unit root in $\rho_{k,t}$ (Baxter and King 1999), which is necessary since $y_{k,t}$ is $I(0)$.

We initialize $\rho_{k,t}$ by using a first-step nonlinear least squares (NLS) procedure, in which we regress $y_{k,t}$ on the seasonal dummy variables, under the restriction that the sum of all parameters is zero. This parameterization ensures that $\sum_{j=1}^{S} \rho_{k,j,1} = 0$. As a consequence, $s_{k,1}$ is centered at zero for each dependent variable (see the Appendix). Alternatives to this initialization may also be considered. However, it transpires that the NLS procedure used for initialization is very useful for the effective estimation of Seasonal-QVAR. Due to this initialization of seasonality, the Seasonal-QVAR specification used in this paper is able to disentangle the dynamic interaction effects measured by μ_t from the stochastic seasonality effects measured by s_t.

In Seasonal-QVAR, the local level component μ_t measures all dynamic interaction effects among y_t. Therefore, we focus on the following structural-form nonlinear VMA(∞) representa-

tion of the local level component (Blazsek, Escribano, and Licht 2017):

$$\mu_t = \sum_{j=0}^{\infty} \Phi^j \Psi[(\nu-2)\nu]^{1/2} \Omega_v^{-1} \frac{\epsilon_{t-1-j}}{\nu - 2 + \epsilon'_{t-1-j}\epsilon_{t-1-j}}. \tag{3}$$

Let C_1 denote the maximum modulus of eigenvalues of Φ. The series in Equation (3) is convergent if $C_1 < 1$. $\text{IRF}_{j,t} = \partial \mu_{t+j} / \partial \epsilon_{t-1}$ is given by (Blazsek, Escribano, and Licht 2017):

$$\text{IRF}_{j,t} = \Phi^j \Psi[(\nu-2)\nu]^{1/2} \Omega_v^{-1} Q_{t-1} \quad \text{for} \quad j = 0, 1, \ldots, \infty, \tag{4}$$

where

$$Q_t = \frac{\partial \frac{\epsilon_t}{\nu - 2 + \epsilon'_t \epsilon_t}}{\partial \epsilon_t} = \begin{bmatrix} q_{1,1,t} & \cdots & q_{1,K,t} \\ \cdots & \cdots & \cdots \\ q_{K,1,t} & \cdots & q_{K,K,t} \end{bmatrix} = \tag{5}$$

$$= \begin{bmatrix} \frac{\nu-2+\epsilon'_t\epsilon_t - 2\epsilon_{1,t}^2}{(\nu-2+\epsilon'_t\epsilon_t)^2} & \frac{-2\epsilon_{1,t}\epsilon_{2,t}}{(\nu-2+\epsilon'_t\epsilon_t)^2} & \cdots & \frac{-2\epsilon_{1,t}\epsilon_{K,t}}{(\nu-2+\epsilon'_t\epsilon_t)^2} \\ \frac{-2\epsilon_{2,t}\epsilon_{1,t}}{(\nu-2+\epsilon'_t\epsilon_t)^2} & \frac{\nu-2+\epsilon'_t\epsilon_t - 2\epsilon_{2,t}^2}{(\nu-2+\epsilon'_t\epsilon_t)^2} & \cdots & \cdots \\ \cdots & \cdots & \cdots & \cdots \\ \frac{-2\epsilon_{K,t}\epsilon_{1,t}}{(\nu-2+\epsilon'_t\epsilon_t)^2} & \cdots & \cdots & \frac{\nu-2+\epsilon'_t\epsilon_t - 2\epsilon_{K,t}^2}{(\nu-2+\epsilon'_t\epsilon_t)^2} \end{bmatrix}.$$

The matrix $Q_t = I_K$ for VARMA and VAR thus the IRF is constant for those models. For QVAR, we use the unconditional mean of $\text{IRF}_{j,t}$ (Blazsek, Escribano, and Licht 2017):

$$\text{IRF}_j = E(\text{IRF}_{j,t}) = \Phi^j \Psi[(\nu-2)\nu]^{1/2} \Omega_v^{-1} E(Q_{t-1}) \quad \text{for} \quad j = 0, 1, 2, \ldots, \infty. \tag{6}$$

If all elements of Q_t are covariance stationary, then $E(Q_{t-1})$ can be estimated by using the sample average (see, for example, Hamilton 1994, Chapter 7.2). We test the covariance stationarity of Q_t by using the augmented Dickey-Fuller (ADF, Dickey and Fuller 1979) test with constant.

We estimate the IRF confidence interval by using 10,000 Monte Carlo simulations from the ML estimates. An alternative to the use of the time-invariant $E(\text{IRF}_{j,t})$ is the period-by-period estimation and analysis of $\text{IRF}_{j,t}$. In those applications, $\text{IRF}_{j,t}$ can be averaged, for example, for pre- and post-oil crisis periods, and the resulting IRF estimates can be compared.

2.2. Statistical inference of Seasonal-QVAR

We estimate Seasonal-QVAR by using the maximum likelihood (ML) method (see, for example, Davidson and MacKinnon 2003). Related to this, we also refer to the works of Creal, Koopman, and Lucas (2013) and Harvey (2013). The ML estimator of parameters is

$$\hat{\Theta}_{\text{ML}} = \arg\max_{\Theta} \text{LL}(y_1, \ldots, y_T; \Theta) = \arg\max_{\Theta} \sum_{t=1}^{T} \ln f(y_t | y_1, \ldots, y_{t-1}; \Theta), \tag{7}$$

where Θ denotes the vector of constant parameters. We use the numerically estimated inverse information matrix for the ML standard errors (Creal, Koopman, and Lucas 2013; Harvey 2013).

We use results from Harvey (2013, Chapters 2.3, 2.4 and 3.3) for the conditions of consistency and asymptotic normality of the ML estimator (see also Blazsek, Escribano, and Licht 2017). Related to the asymptotic properties of ML, we also study the invertibility of Seasonal-QVAR (see, for example, Blasques, Gorgi, Koopman, and Wintenberger 2018).

First, Condition 1 is $C_1 < 1$ hence μ_t is covariance stationary. Second, Condition 2 holds if $E[u_{j,t}^{2-i}(\partial u_{k,t}/\partial \mu_{l,t})^i] < \infty$, where $i = 0, 1, 2$ and $j, k, l = 1, \ldots, K$ (we use the sample average to estimate this expectation that we support by the ADF test). Third, for Condition 3 we consider the representative element $\Psi_{i,j}$ from the matrix Ψ. From the dynamic local level equation $\mu_t = \Phi\mu_{t-1} + \Psi u_{t-1}$, we express

$$\frac{\partial \mu_t}{\partial \Psi_{i,j}} = \Phi \frac{\partial \mu_{t-1}}{\partial \Psi_{i,j}} + \Psi \frac{\partial u_{t-1}}{\partial \Psi_{i,j}} + W_{i,j} u_{t-1} \tag{8}$$

for all $t = 1, \ldots, T$, where the element (i, j) of the matrix $W_{i,j}$ $(K \times K)$ is one and the rest of

the elements of $W_{i,j}$ are zero. By using the chain rule, we can also write Equation (8) as

$$\frac{\partial \mu_t}{\partial \Psi_{i,j}} = \left(\Phi + \Psi \frac{\partial u_{t-1}}{\partial \mu'_{t-1}} \right) \frac{\partial \mu_{t-1}}{\partial \Psi_{i,j}} + W_{i,j} u_{t-1} = X_t \frac{\partial \mu_{t-1}}{\partial \Psi_{i,j}} + W_{i,j} u_{t-1}. \tag{9}$$

Condition 3 is that all eigenvalues of $E(X_t)$ are within the unit circle, where the finiteness of all elements of $E(X_t)$ follows from Condition 2. We denote the maximum modulus of eigenvalues of $E(X_t)$ by using C_3. If each element of X_t is covariance stationary, then $E(X_t)$ can be estimated by using the sample average (we support the use of this estimator by the ADF test). Fourth, for Condition 4, we consider that the information matrix depends on:

$$\frac{\partial \mu_t}{\partial \Psi_{i,j}} \frac{\partial \mu'_t}{\partial \Psi_{k,l}} = X_t \frac{\partial \mu_{t-1}}{\partial \Psi_{i,j}} \frac{\partial \mu'_{t-1}}{\partial \Psi_{k,l}} X'_t + X_t \frac{\partial \mu_{t-1}}{\partial \Psi_{i,j}} W'_{i,j} u_{t-1} + u'_{t-1} W_{k,l} \frac{\partial \mu'_{t-1}}{\partial \Psi_{k,l}} X'_t + W_{i,j} u_{t-1} u'_{t-1} W'_{k,l} \tag{10}$$

that we can also write as

$$\begin{aligned} \text{vec}\left(\frac{\partial \mu_t}{\partial \Psi_{i,j}} \frac{\partial \mu'_t}{\partial \Psi_{k,l}} \right) &= (X_t \otimes X_t) \text{vec}\left(\frac{\partial \mu_{t-1}}{\partial \Psi_{i,j}} \frac{\partial \mu'_{t-1}}{\partial \Psi_{k,l}} \right) + \\ &+ \text{vec}\left(X_t \frac{\partial \mu_{t-1}}{\partial \Psi_{i,j}} W'_{i,j} u_{t-1} \right) + \text{vec}\left(u'_{t-1} W_{k,l} \frac{\partial \mu'_{t-1}}{\partial \Psi_{k,l}} X'_t \right) + \text{vec}\left(W_{i,j} u_{t-1} u'_{t-1} W'_{k,l} \right), \end{aligned} \tag{11}$$

where $\otimes$ is the Kronecker product and vec(x) indicates that the columns of the matrix are being stacked one upon the other. Condition 4 is that all eigenvalues of $E(X_t \otimes X_t)$ are within the unit circle, where the finiteness of all elements of $E(X_t \otimes X_t)$ follows from Condition 2. We denote the maximum modulus of eigenvalues of $E(X_t \otimes X_t)$ by using C_4. If each element of $X_t \otimes X_t$ is covariance stationary, then $E(X_t \otimes X_t)$ can be estimated by using the sample average (we support the use of this estimator by the ADF test). For the computation of $X_t = \Phi + \Psi(\partial u_{t-1}/\partial \mu'_{t-1})$ in Conditions 3 and 4, we use the formula for $\partial u_t / \partial \mu'_t$ $(K \times K)$. As aforementioned, the score function is given by

$$u_t = \left(1 + \frac{v'_t \Sigma_v^{-1} v_t}{\nu} \right)^{-1} v_t = \frac{\nu (y_t - c - \mu_t - s_t)}{\nu + (y_t - c - \mu_t - s_t)' \Sigma_v^{-1} (y_t - c - \mu_t - s_t)} \tag{12}$$

and the formula of $\partial u_t / \partial \mu_t'$ can be obtained by using standard matrix calculus.

In addition to the previous conditions, we also study the invertibility of Seasonal-QVAR that is a condition of the consistency and asymptotic normality of ML. Invertibility is studied in the recent literature on DCS models (see for example: Blasques, Gorgi, Koopman, and Wintenberger 2018). From equations $y_t = c + \mu_t + s_t + v_t$ and $\mu_t = \Phi \mu_{t-1} + \Psi u_{t-1}$, we express:

$$y_t = (I_K - \Phi)c + \Phi y_{t-1} + (I_K - \Phi L)s_t - \Phi v_{t-1} + \Psi u_{t-1} + v_t. \tag{13}$$

We substitute the score function into the previous equation and obtain:

$$y_t = (I_K - \Phi)c + \Phi y_{t-1} + (I_K - \Phi L)s_t + \frac{\Psi\nu - \Phi}{\nu + v_{t-1}'\Sigma_v^{-1}v_{t-1}} v_{t-1} + v_t. \tag{14}$$

This equation is a Seasonal-VARMA(1,1) model, for which the MA(1) parameter is observation-driven, and it is defined as: $\Psi_t = (\Psi\nu - \Phi)/(\nu + v_{t-1}'\Sigma_v^{-1}v_{t-1})$. VARMA(1,1) with constant parameters is invertible if the maximum modulus of eigenvalues of the MA(1) parameter is less than one. We study this condition for Ψ_t for $t = 1, \ldots, T$.

Finally, for the seasonality component s_t, the conditions of ML are satisfied if the parameters of $\rho_{k,t-1}$ are set to the identity matrix (i.e., multivariate random walk), as in the equation $\rho_{k,t} = \rho_{k,t-1} + \gamma_{k,t} u_{k,t-1}$. If the unit root is imposed rather than estimated in DCS models of trend or seasonality, then standard asymptotics of ML do apply.

2.3. Gaussian Seasonal-VARMA

Seasonal-QVAR can be related to the Gaussian Seasonal-VARMA and Gaussian Seasonal-VAR models. With respect to VAR, we refer to the works of Sims (1980, 1986), Sims, Goldfeld, and Sachs (1982), Bernanke (1986), Blanchard and Watson (1986), and Stock and Watson (2001). With respect to VARMA, we refer to the seminal paper of Tiao and Tsay (1989). We also refer to the related textbooks of Hamilton (1994, Chapters 10 to 12) and Lütkepohl (2005).

If $\nu \to \infty$, then $v_t \to_d N_K(0, \Sigma_v)$ and $u_t \to_p v_t$ (see Equation (12)). From equations

$y_t = c + \mu_t + s_t + v_t$ and $\mu_t = \Phi\mu_{t-1} + \Psi u_{t-1}$, we obtain the Gaussian Seasonal-QVAR model:

$$y_t = (I_K - \Phi)c + \Phi y_{t-1} + (I_K - \Phi L)s_t + (\Psi - \Phi)v_{t-1} + v_t, \tag{15}$$

where L denotes the lag operator. Thus, Seasonal-QVAR becomes Gaussian Seasonal-VARMA, in which the error term v_t has a multivariate i.i.d. Gaussian distribution and both local level μ_t and stochastic seasonality s_t are updated by v_{t-1}. Gaussian Seasonal-VARMA is a special case of Seasonal-QVAR for large ν. Furthermore, Gaussian Seasonal-VAR is another special case of Seasonal-QVAR for large ν and $\Psi = \Phi$. In this paper, we focus on the Gaussian Seasonal-VARMA alternative.

For Seasonal-VARMA, the local level μ_t measures all dynamic interaction effects among y_t. Therefore, we focus on the VMA(∞) representation $\mu_t = \sum_{j=0}^{\infty} \Phi^j \Psi \Omega_v^{-1} \epsilon_{t-1-j}$, which is obtained by using the decomposition $\Sigma_v = \Omega_v^{-1}(\Omega_v^{-1})'$. Let C_1 denote the maximum modulus of eigenvalues of Φ. If $C_1 < 1$, then the series in the VMA(∞) representation is finite. For Seasonal-VARMA, $\text{IRF}_{j,t} = \partial\mu_{t+j}/\partial\epsilon_{t-1} = \Phi^j \Psi \Omega_v^{-1}$ for $j = 0, 1, \ldots, \infty$.

We estimate Seasonal-VARMA by using the ML method. Even if the $v_t \sim N_K(0, \Sigma_v)$ assumption does not hold, the ML estimator still provides consistent parameter estimates for Seasonal-VARMA according to the quasi-ML (QML) results of Gouriéroux, Monfort, and Trognon (1984). We denote the maximum moduli of eigenvalues of Φ and $\Psi - \Phi$ with C_1 and C_2, respectively. For Seasonal-VARMA, $C_1 < 1$ and $C_2 < 1$ ensure that ML is consistent and asymptotically normal.

2.4. Basic structural model

The basic structural model is $y_t = c + \mu_t + s_t + v_t$, where c $(K \times 1)$ includes constant parameters, μ_t $(K \times 1)$ is the local level component, s_t $(K \times 1)$ is the stochastic seasonality component, and $v_t \sim N_K(0_{K\times 1}, \Sigma_v)$ is a multivariate i.i.d. Gaussian error term. The positive definite covariance matrix is decomposed as $\Sigma_v = \Omega_v^{-1}(\Omega_v^{-1})'$. We formulate the local level component as $\mu_t = \Phi\mu_{t-1} + \eta_t$, where Φ $(K \times K)$ is a constant parameter matrix, and $\eta_t \sim N_K(0_{K\times 1}, \Sigma_\eta)$

is the multivariate i.i.d. reduced-form error term. The covariance matrix is decomposed as $\Sigma_\eta = \Omega_\eta^{-1}(\Omega_\eta^{-1})'$, and we introduce the multivariate i.i.d. structural-form error term $\epsilon_t = \Omega_\eta \eta_t$. We initialize μ_t in the same way as for Seasonal-QVAR. We formulate each element of the seasonality component $s_t = (s_{1,t}, \ldots, s_{K,t})'$ according to the product $s_{k,t} = D_t' \rho_{k,t}$ for each $k = 1, \ldots, K$, where D_t $(S \times 1)$ is a vector of seasonal dummy variables and $\rho_{k,t}$ $(S \times 1)$ is a vector of dynamic seasonality parameters. Variable ρ_{kt} is updated according to the dynamic equation $\rho_{k,t} = \rho_{k,t-1} + \xi_{k,t}$, where $\xi_{k,t} \sim N_S(0, \Sigma_{\xi,k})$ is a multivariate i.i.d. Gaussian error term. We ensure that $s_{k,t}$ is centered at zero by using the specification $\Sigma_{\xi,k} = \sigma_{\xi,k}(I_S - i_S i_S'/S)$, where $\sigma_{\xi,k}$ is a positive parameter and i_S denotes a $S \times 1$ vector of ones. We initialize $\rho_{k,t}$ by using the same first-step NLS procedure that is used for Seasonal-QVAR.

For the basic structural model estimated in this paper, the local level component μ_t measures all dynamic interaction effects among y_t. Therefore, we focus on the following VMA(∞) representation: $\mu_t = \sum_{j=0}^{\infty} \Phi^j \Omega_\eta^{-1} \epsilon_{t-j}$. Let C_1 denote the maximum modulus of eigenvalues of Φ. If $C_1 < 1$, then $\text{IRF}_{j,t} = \partial \mu_{t+j} / \partial \epsilon_t = \Phi^j \Omega_\eta^{-1}$ for $j = 0, 1, \ldots, \infty$.

We estimate the basic structural model by using the ML method, for which the likelihood function is computed by using the Kalman filtering technique (Kalman 1960; Harvey 1989).

3. Application to world crude oil production and global real economic activity

3.1. Classic macroeconomic dataset

We use monthly time series data from world crude oil production growth $y_{1,t}$, and a business cycle index measuring global real economic activity growth $y_{2,t}$, for the period of March 1973 to December 2007. The source of these data is the book of Kilian and Lütkepohl (2017) (the data are downloaded from: http://www-personal.umich.edu/~lkilian/figure12_7.zip). As aforementioned, the use of those variables is motivated by several works that study the question of how changes in supply and demand in the world crude oil market are related to economic growth (i.e., Blanchard 2002; Barsky and Kilian 2002, 2004; Hamilton 2003; Kilian 2008, 2009; Baumeister and Hamilton 2017; Kilian and Lütkepohl 2017). World crude oil production has a significant annual seasonality component: During the summer months supply exceeds demand

(i.e., relatively high crude oil production), while during the winter months demand exceeds supply (i.e., relatively low crude oil production) (Ye, Zyren, and Shore 2006). The global real economic activity variable of the present paper is developed by Kilian (2009), who uses dry cargo single voyage ocean freight rates to measure global real economic activity. The work of Kilian (2009) motivates the use of the ocean freight rate-based global real economic activity index. Ocean freight rates have a significant seasonality component, with a period of about six months (Raunglerdpanyagul 1985).

In our application, $y_t = (y_{1,t}, y_{2,t})'$ (thus, for the multivariate models of this paper $K = 2$), and we use the seasonal dummies $D_t = (D_{\text{Jan},t}, \ldots, D_{\text{Dec},t})'$ (thus, the period of the annual seasonality used in this paper is $S = 12$). For $y_{1,t}$ and $y_{2,t}$, descriptive statistics and ADF with constant test results are reported in Table 1. Heteroscedasticity and autocorrelation consistent (HAC) ordinary least squares (OLS) estimates (Newey and West 1987) of a linear regression of $y_{1,t}$ and $y_{2,t}$ on monthly dummies are also reported in Table 1, which suggest that both variables may have seasonality components.

Motivated by the work of Kilian and Lütkepohl (2017, Chapter 12.13.1), all multivariate dynamic models of the dataset used in this paper are recursively identified. Therefore, Σ_v for Seasonal-QVAR and Seasonal-VARMA is decomposed according to the Cholesky decomposition. Similarly, Σ_v and Σ_η for the basic structural model are also decomposed according to the Cholesky decomposition.

Table 1
Descriptive statistics.

Panel A. Descriptive statistics	World crude oil production growth $y_{1,t}$	Global real economic activity growth $y_{2,t}$
Start date	March 1973	March 1973
End date	December 2007	December 2007
Sample size T	418	418
Minimum	−9.9073	−20.8529
Maximum	6.4986	17.0466
Mean	0.0719	0.0497
Standard deviation	1.7117	4.8134
Skewness	−1.5326	−0.2381
Excess kurtosis	8.1718	1.8608
ADF	-22.3144^{***}	-15.2541^{***}
Panel B. Seasonality effects	**World crude oil production growth y_{1t}**	**Global real economic activity growth y_{2t}**
δ_{Jan}	$-1.2007^{***}(0.4342)$	$-2.0955^{***}(0.768)$
δ_{Feb}	$0.3447(0.3137)$	$-1.0236(0.6247)$
δ_{Mar}	$0.0716(0.1882)$	$2.0131^{**}(0.8216)$
δ_{Apr}	$-0.2675(0.202)$	$-0.4418(0.6527)$
δ_{May}	$-0.1369(0.2217)$	$1.248(0.7759)$
δ_{Jun}	$0.1075(0.2525)$	$-2.9096^{***}(0.8132)$
δ_{Jul}	$0.7465^{***}(0.257)$	$-2.8145^{***}(0.7816)$
δ_{Aug}	$-0.213(0.2634)$	$0.2747(0.6942)$
δ_{Sep}	$0.5944^{*}(0.3122)$	$3.0974^{***}(0.6693)$
δ_{Oct}	$0.3188(0.3721)$	$2.8003^{***}(0.7255)$
δ_{Nov}	$0.3663^{*}(0.2105)$	$1.853^{***}(0.5436)$
δ_{Dec}	$0.1032(0.2071)$	$-1.4976^{*}(0.888)$

Growth in variables is measured in percentage points. Robust standard errors are in parentheses. *, ** and *** indicate significance at the 10%, 5% and 1% levels, respectively.

3.2. Detecting seasonality with QVAR

In this section, we consider that the data generating process (DGP) includes a seasonality component that we would like to disentangle from the local level component. For the extreme case where seasonality is not specified in QVAR (i.e., $y_t = c + \mu_t + v_t$, where each component is specified as in Section 2.1), we show that dynamic seasonality effects will appear in the local level component. This is indicated by the fact that seasonality effects will be observed in the IRF of μ_t. Thus, for a given Seasonal-QVAR specification, the IRF is a useful tool that analyzes the effectiveness of information disentanglement for μ_t and s_t. If the IRF does not indicate seasonality dynamics, then s_t will capture all seasonality effects and the disentanglement of μ_t and s_t is effective.

We first present the parameter estimates and model diagnostics of QVAR (i.e., $y_t = c+\mu_t+v_t$, where each component is specified as in Section 2.1) in Table 2. This table indicates that we

are not able to estimate QVAR for the case where all elements of Ψ are estimated ('Ψ full' in Table 2), as the ML estimator does not converge to an optimum. We are able to estimate QVAR for the restricted case, where Ψ is a diagonal matrix ('Ψ diagonal' in Table 2) (for that specification, ML is supported by C_1 to C_4, and the MDS test does not reject the specifications of ϵ_t and u_t; Table 2). We present the IRF of μ_t for QVAR with Ψ diagonal in Fig. 1, where the IRF estimates indicate seasonality effects in μ_t. These findings suggest that for Seasonal-QVAR the effectiveness of disentanglement of the local level and the stochastic seasonality components can be analyzed by using the IRF tool.

We also show in this section, for the extreme case where the seasonality component is not included in VARMA (i.e., $y_t = c + \mu_t + v_t$, where each component is specified as in Section 2.3), that seasonality effects will not appear in the local level component of the model (i.e., seasonality effects will not be observed in the IRF of μ_t). We present the parameter estimates and diagnostics of VARMA in Table 2 and the corresponding IRF in Fig. 1. We estimate VARMA with the Ψ full and also with the Ψ diagonal specifications (C_1 and C_2 support the asymptotic properties of QML for VARMA, and the MDS test does not reject the specification of ϵ_t; Table 2). We find that the statistical performance of VARMA is inferior to that of QVAR, according to the LL, Akaike information criterion (AIC), Bayesian information criterion (BIC) and Hannan–Quinn criterion (HQC) metrics (see, for example, Davidson and MacKinnon 2003) (Table 2). More importantly, although the DGP includes a seasonality component the related seasonality effects do not appear in the IRF of VARMA (Fig. 1). As a consequence, for Seasonal-VARMA, the effectiveness of the disentanglement of μ_t and s_t cannot be analyzed by using the IRF tool.

Table 2
Parameter estimates and model diagnostics (QVAR; VARMA).

	QVAR Ψ full	QVAR Ψ diagonal	VARMA Ψ full	VARMA Ψ diagonal
c_1	NA	$0.1740^{***}(0.0571)$	$0.0337(0.0261)$	$0.0247(0.0163)$
c_2	NA	$0.0915(0.2618)$	$0.1491(0.2685)$	$0.0515(0.2587)$
$\Phi_{1,1}$	NA	$-0.7282^{***}(0.2123)$	$0.5557^{***}(0.1164)$	$0.6461^{***}(0.0830)$
$\Phi_{1,2}$	NA	$0.0983^{*}(0.0525)$	$-0.0191(0.0340)$	$0.0151^{*}(0.0084)$
$\Phi_{2,1}$	NA	$-2.0782(1.6415)$	$-1.4298^{*}(0.7634)$	$-0.0363(0.1169)$
$\Phi_{2,2}$	NA	$0.4562^{***}(0.1494)$	$0.2133(0.1520)$	$0.1214^{**}(0.0555)$
$\Psi_{1,1}$	NA	$0.0593(0.0798)$	$-0.7243^{***}(0.1021)$	$-0.8129^{***}(0.0640)$
$\Psi_{1,2}$	NA	NA	$0.0451(0.0460)$	NA
$\Psi_{2,1}$	NA	NA	$1.4934^{*}(0.7819)$	NA
$\Psi_{2,2}$	NA	$0.6794^{***}(0.1147)$	$0.0753(0.1510)$	$0.1745^{***}(0.0544)$
$\Omega_{v,1,1}^{-1}$	NA	$1.0391^{***}(0.0556)$	$1.6717^{***}(0.0569)$	$1.6727^{***}(0.0549)$
$\Omega_{v,2,1}^{-1}$	NA	$0.1906(0.1799)$	$0.4147^{*}(0.2169)$	$0.4099^{**}(0.1948)$
$\Omega_{v,2,2}^{-1}$	NA	$3.2280^{***}(0.1685)$	$4.5593^{***}(0.1527)$	$4.5856^{***}(0.1176)$
ν	NA	$3.0951^{***}(0.3974)$	NA	NA
C_1	NA	0.5187	0.6224	0.6450
C_2	NA	NA	0.8011	0.8129
C_2 to C_4 ADF	NA	All stationary	NA	NA
C_3	NA	0.4638	NA	NA
C_4	NA	0.2160	NA	NA
Q_t ADF	NA	All stationary	NA	NA
MDS $\epsilon_{1,t}$	NA	0.2127	0.6693	0.6695
MDS $\epsilon_{2,t}$	NA	0.1559	0.9983	0.9763
MDS $u_{1,t}$	NA	0.7120	NA	NA
MDS $u_{2,t}$	NA	0.9384	NA	NA
LL	NA	**−4.6943**	−4.8689	−4.8752
AIC	NA	**9.4460**	9.8000	9.8031
BIC	NA	**9.5619**	9.9255	9.9093
HQC	NA	**9.4918**	9.8496	9.8450

For all models presented in this table, y_t is decomposed as

$$\begin{bmatrix} y_{1,t} \\ y_{2,t} \end{bmatrix} = \begin{bmatrix} c_1 \\ c_2 \end{bmatrix} + \begin{bmatrix} \mu_{1,t} \\ \mu_{2,t} \end{bmatrix} + \begin{bmatrix} v_{1,t} \\ v_{2,t} \end{bmatrix}$$

QVAR Ψ diagonal:

$$\begin{bmatrix} \mu_{1,t} \\ \mu_{2,t} \end{bmatrix} = \begin{bmatrix} \Phi_{1,1} & \Phi_{1,2} \\ \Phi_{2,1} & \Phi_{2,2} \end{bmatrix} \begin{bmatrix} \mu_{1,t-1} \\ \mu_{2,t-1} \end{bmatrix} + \begin{bmatrix} \Psi_{1,1} & 0 \\ 0 & \Psi_{2,2} \end{bmatrix} \begin{bmatrix} u_{1,t-1} \\ u_{2,t-1} \end{bmatrix}$$

$$\begin{bmatrix} u_{1,t} \\ u_{2,t} \end{bmatrix} = \left\{ 1 + \tfrac{1}{\nu}(v_{1,t}, v_{2,t}) \left[\begin{pmatrix} \Omega_{v,1,1}^{-1} & 0 \\ \Omega_{v,2,1}^{-1} & \Omega_{v,2,2}^{-1} \end{pmatrix} \begin{pmatrix} \Omega_{v,1,1}^{-1} & \Omega_{v,2,1}^{-1} \\ 0 & \Omega_{v,2,2}^{-1} \end{pmatrix} \right]^{-1} \begin{pmatrix} v_{1,t} \\ v_{2,t} \end{pmatrix} \right\}^{-1} \begin{pmatrix} v_{1,t} \\ v_{2,t} \end{pmatrix}$$

VARMA Ψ full:

$$\begin{bmatrix} \mu_{1,t} \\ \mu_{2,t} \end{bmatrix} = \begin{bmatrix} \Phi_{1,1} & \Phi_{1,2} \\ \Phi_{2,1} & \Phi_{2,2} \end{bmatrix} \begin{bmatrix} \mu_{1,t-1} \\ \mu_{2,t-1} \end{bmatrix} + \begin{bmatrix} \Psi_{1,1} & \Psi_{1,2} \\ \Psi_{2,1} & \Psi_{2,2} \end{bmatrix} \begin{bmatrix} v_{1,t-1} \\ v_{2,t-1} \end{bmatrix}$$

VARMA Ψ diagonal:

$$\begin{bmatrix} \mu_{1,t} \\ \mu_{2,t} \end{bmatrix} = \begin{bmatrix} \Phi_{1,1} & \Phi_{1,2} \\ \Phi_{2,1} & \Phi_{2,2} \end{bmatrix} \begin{bmatrix} \mu_{1,t-1} \\ \mu_{2,t-1} \end{bmatrix} + \begin{bmatrix} \Psi_{1,1} & 0 \\ 0 & \Psi_{2,2} \end{bmatrix} \begin{bmatrix} v_{1,t-1} \\ v_{2,t-1} \end{bmatrix}$$

Not available (NA). We are not able to estimate QVAR 'Ψ full', as the ML estimator does not converge to an optimum. 'MDS' denotes the p-value of the martingale difference sequence test. Bold numbers indicate superior model performance. C_1 and C_2 are the maximum moduli of eigenvalues of Φ and Ψ, respectively. C_3 and C_4 are the maximum moduli of eigenvalues of $\hat{E}(X_t)$ and $\hat{E}(X_t \otimes X_t)$, respectively. We summarize ADF results for Conditions 2 to 4 and matrix Q_t, by using 'All stationary'. Standard errors are in parentheses. *, ** and *** indicate significance at the 10%, 5% and 1% levels, respectively.

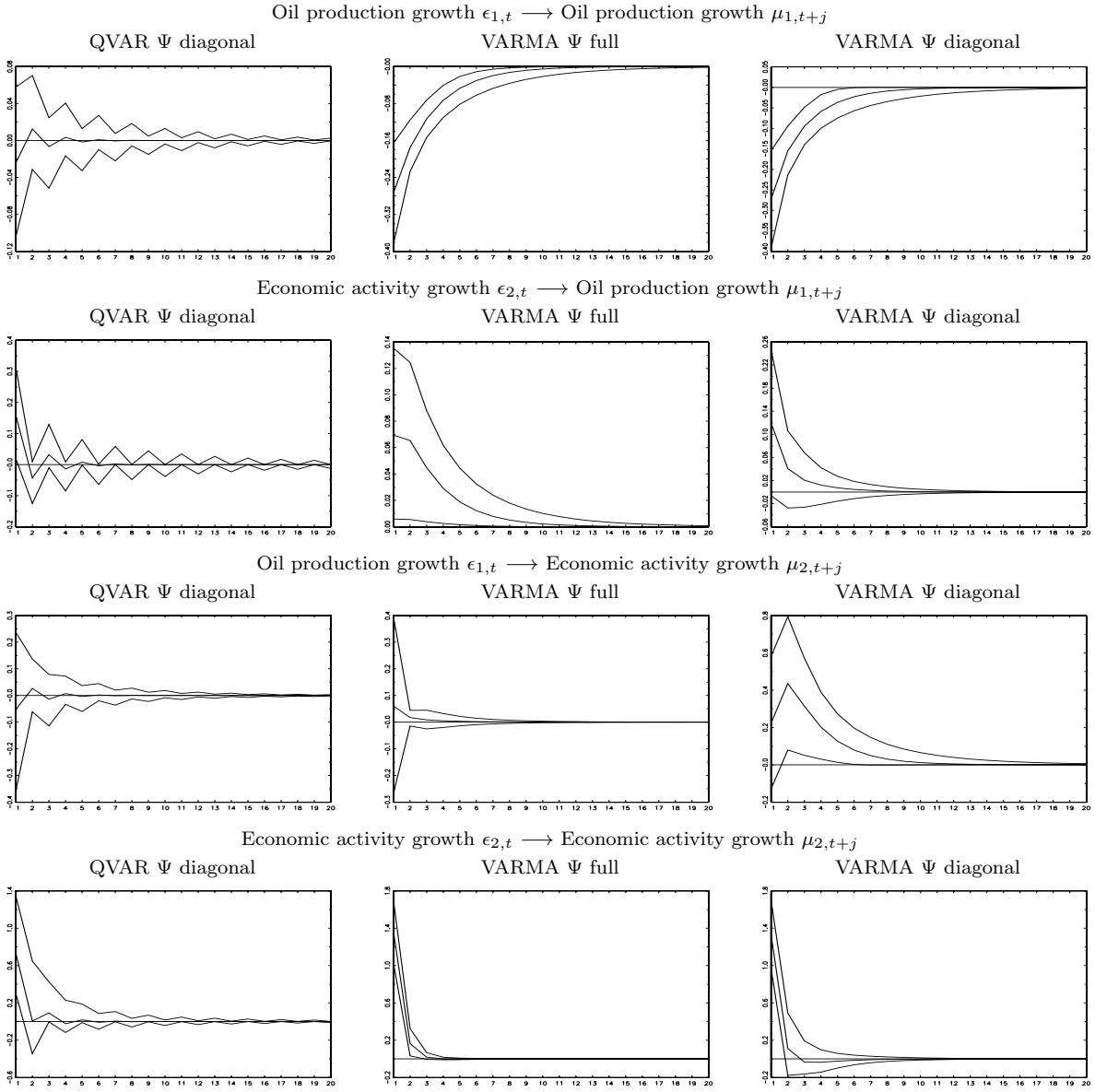

Fig. 1. Impulse response function with 90% confidence interval (QVAR; VARMA).
The IRF confidence interval is estimated by using 10,000 Monte Carlo simulations from the ML estimates.

3.3. Empirical results

In this section, we report results for the joint estimation of local level, seasonality and irregular components. We present the parameter estimates and model diagnostics for Seasonal-QVAR and the basic structural model in Table 3. We present the parameter estimates and model diagnostics for Gaussian Seasonal-VARMA in Table 4. For Seasonal-QVAR, we study the condition of invertibility in Fig. 2. We present the time series components of Seasonal-QVAR, the basic structural model and Gaussian Seasonal-VARMA in Figs. 3 to 5, respectively. We present the

IRF estimates for all models in Fig. 6, and we demonstrate that Seasonal-QVAR is robust to extreme observations in Fig. 7.

Consistency and asymptotic normality of the estimates are supported by C_1, C_2, C_3 or C_4 for each model (Tables 3 and 4). For Seasonal-QVAR, we present the evolution of the maximum modulus of eigenvalues of Ψ_t in Fig. 2. The average value of Ψ_t for the sample period is 0.7567, which suggests that Seasonal-QVAR is invertible. Nevertheless, Fig. 2 also shows that the mean of Ψ_t has a nonlinear increasing trend. Motivated by this, we present the fitted values of a linear regression with quadratic trend and the corresponding robust estimates of the 90% confidence interval for the level in Fig. 2. Those estimates suggest that Seasonal-QVAR is invertible.

We also use the Escanciano–Lobato (2009) martingale difference sequence (MDS) test for ϵ_t and u_t of Seasonal-QVAR and v_t of the basic structural model. We find that MDS is never rejected (Table 3). We use the same MDS test for v_t of Seasonal-VARMA. We find that MDS is never rejected (Table 4).

We compare statistical performances by using the LL, AIC, BIC and HQC metrics. LL and AIC indicate improvement in the model performance of Seasonal-QVAR, with respect to the basic structural model (Table 3). However, BIC and HQC indicate a superior performance for the basic structural model (Table 3). Thus, the basic structural model might be more parsimonious than Seasonal-QVAR. For Gaussian Seasonal-VARMA, we also report the LL, AIC, BIC and HQC metrics (Table 4). Those results indicate that the statistical performance of Seasonal-QVAR is superior to that of the Gaussian Seasonal-VARMA model.

It is noteworthy that LL of QVAR is superior to that of Seasonal-QVAR (see Tables 2 and 3). This result might seem surprising, as one might believe that QVAR is a nested alternative to Seasonal-QVAR. In fact, QVAR is not a special case of the Seasonal-QVAR model that is estimated in this paper, since we use a specific restriction for Seasonal-QVAR on the initial value of $\rho_{k,t}$ that is estimated in the first-step NLS procedure. QVAR is estimated without such a restriction. Nevertheless, as aforementioned, the restriction on the initial value of $\rho_{k,t}$ is important for the effective disentanglement of μ_t and s_t in Seasonal-QVAR.

The estimates of $s_{1,t}$ and $s_{2,t}$ in Figs. 3 to 5 indicate significant seasonality effects with dynamic amplitude for all models, which support the use of stochastic seasonality. The local level estimates $\mu_{1,t}$ and $\mu_{2,t}$ are relatively homogeneous for Seasonal-QVAR compared to the Gaussian alternatives (Figs. 3 to 5). This result suggests that extreme observations tend to appear in the error term of Seasonal-QVAR, while extreme observations sometimes appear in the local level components of the basic structural model and Seasonal-VARMA.

We study interaction effects between world crude oil production growth and global real economic activity growth by using the IRF (Fig. 6). The results are similar for Seasonal-QVAR, the basic structural model and Seasonal-VARMA, and they show that seasonality does not appear in the IRF of μ_t. This point is important for Seasonal-QVAR, since it indicates that the specification applied in this paper effectively disentangles μ_t and s_t.

For Seasonal-QVAR, the score function $u_t = (u_{1t}, u_{2t})'$ discounts extreme values from the structural-form error term $\epsilon_t = (\epsilon_{1t}, \epsilon_{2t})'$. In Fig. 7, we present each element of the updating vector $u_t = (u_{1t}, u_{2t})'$ of Seasonal-QVAR, as a function of ϵ_{1t} and ϵ_{2t}. This figure indicates that both elements of the score function converge to finite values, when either of $|\epsilon_{1t}|$ or $|\epsilon_{2t}|$ goes to infinity. Thus, for Seasonal-QVAR, the score function discounts the influence of extreme values in the noise. To compare the discounting property of the updating terms for Seasonal-QVAR and Seasonal-VARMA, in Fig. 7 we also present each element of the updating vector $v_t = (v_{1t}, v_{2t})'$ of Seasonal-VARMA, as a function of ϵ_{1t} and ϵ_{2t}. This figure indicates that v_{1t} and v_{2t} converge to infinity, when $|\epsilon_{1t}|$ and $|\epsilon_{2t}|$ go to infinity. Thus, for Seasonal-VARMA, the updating terms v_{1t} and v_{2t} do not discount the influence of extreme values in the noise.

Table 3

Parameter estimates and model diagnostics (Seasonal-QVAR; basic structural model).

Seasonal-QVAR				Basic structural model	
c_1	0.1597***(0.0522)	$\gamma_{2,\text{Jan}}$	−0.3705***(0.0679)	c_1	0.0862(0.2706)
c_2	0.1719(0.1723)	$\gamma_{2,\text{Feb}}$	−0.2669***(0.0455)	c_2	0.1215(0.4161)
$\Phi_{1,1}$	0.3935**(0.1725)	$\gamma_{2,\text{Mar}}$	−0.0590**(0.0248)	$\Phi_{1,1}$	−0.0947(0.0599)
$\Phi_{1,2}$	0.0417(0.0280)	$\gamma_{2,\text{Apr}}$	0.1543***(0.0380)	$\Phi_{1,2}$	0.0316(0.0373)
$\Phi_{2,1}$	−0.5042(0.3489)	$\gamma_{2,\text{May}}$	0.0530***(0.0199)	$\Phi_{2,1}$	−0.1555(0.3768)
$\Phi_{2,2}$	0.4989***(0.0867)	$\gamma_{2,\text{Jun}}$	0.4799***(0.0696)	$\Phi_{2,2}$	0.5844***(0.1717)
$\Psi_{1,1}$	−1.0911(0.6638)	$\gamma_{2,\text{Jul}}$	−0.1970***(0.0289)	$\Omega^{-1}_{v,1,1}$	0.2546(0.4974)
$\Psi_{1,2}$	−0.0104(0.0366)	$\gamma_{2,\text{Aug}}$	−0.1387***(0.0392)	$\Omega^{-1}_{v,2,1}$	−3.1755***(0.5416)
$\Psi_{2,1}$	0.7832***(0.2367)	$\gamma_{2,\text{Sep}}$	0.0235(0.0220)	$\Omega^{-1}_{v,2,2}$	0.0124***(0.0003)
$\Psi_{2,2}$	0.7953***(0.1033)	$\gamma_{2,\text{Oct}}$	0.2720***(0.0962)	$\Omega^{-1}_{\eta,1,1}$	1.5925***(0.0916)
$\Omega^{-1}_{v,1,1}$	1.1981***(0.0587)	$\gamma_{2,\text{Nov}}$	0.0595(0.0403)	$\Omega^{-1}_{\eta,2,1}$	0.6450(0.9284)
$\Omega^{-1}_{v,2,1}$	−0.4530**(0.1863)	$\gamma_{2,\text{Dec}}$	0.2695***(0.0568)	$\Omega^{-1}_{\eta,2,2}$	2.3133***(0.8054)
$\Omega^{-1}_{v,2,2}$	3.1445***(0.1471)	C_1	0.4662	$\sigma_{\xi,1}$	0.0413***(0.0138)
ν	3.4490***(0.4395)	C_2 to C_4 ADF	All stationary	$\sigma_{\xi,2}$	0.0697**(0.0322)
$\gamma_{1,\text{Jan}}$	−0.3368(0.7437)	C_3	0.4365	C_1	0.5770
$\gamma_{1,\text{Feb}}$	1.1408(0.7980)	C_4	0.2359	MDS $v_{1,t}$	0.9328
$\gamma_{1,\text{Mar}}$	1.2451*(0.7206)	Q_t ADF	All stationary	MDS $v_{2,t}$	0.6402
$\gamma_{1,\text{Apr}}$	−0.5284(0.7919)	MDS $v_{1,t}$	0.6641	LL	−4.8033
$\gamma_{1,\text{May}}$	0.9586(0.7120)	MDS $v_{2,t}$	0.5471	AIC	9.6735
$\gamma_{1,\text{Jun}}$	0.6592(0.7698)	MDS $u_{1,t}$	0.3520	BIC	**9.8087**
$\gamma_{1,\text{Jul}}$	0.5037(0.7483)	MDS $u_{2,t}$	0.1269	HQC	**9.7269**
$\gamma_{1,\text{Aug}}$	0.8943(0.8526)	LL	**-4.7442**		
$\gamma_{1,\text{Sep}}$	0.3072(0.6873)	AIC	**9.6702**		
$\gamma_{1,\text{Oct}}$	2.8221***(0.8270)	BIC	10.0371		
$\gamma_{1,\text{Nov}}$	0.6534(0.7598)	HQC	9.8153		
$\gamma_{1,\text{Dec}}$	0.6847(0.7181)				

For all models presented in this table, y_t is decomposed as

$$\begin{bmatrix} y_{1,t} \\ y_{2,t} \end{bmatrix} = \begin{bmatrix} c_1 \\ c_2 \end{bmatrix} + \begin{bmatrix} \mu_{1,t} \\ \mu_{2,t} \end{bmatrix} + \begin{bmatrix} s_{1,t} \\ s_{2,t} \end{bmatrix} + \begin{bmatrix} v_{1,t} \\ v_{2,t} \end{bmatrix}$$

Seasonal-QVAR:

$$\begin{bmatrix} \mu_{1,t} \\ \mu_{2,t} \end{bmatrix} = \begin{bmatrix} \Phi_{1,1} & \Phi_{1,2} \\ \Phi_{2,1} & \Phi_{2,2} \end{bmatrix} \begin{bmatrix} \mu_{1,t-1} \\ \mu_{2,t-1} \end{bmatrix} + \begin{bmatrix} \Psi_{1,1} & \Psi_{1,2} \\ \Psi_{2,1} & \Psi_{2,2} \end{bmatrix} \begin{bmatrix} u_{1,t-1} \\ u_{2,t-1} \end{bmatrix}$$

$$\begin{bmatrix} s_{1,t} \\ s_{2,t} \end{bmatrix} = \begin{bmatrix} D_t'\rho_{1,t} \\ D_t'\rho_{2,t} \end{bmatrix} = \begin{bmatrix} D_t'(\rho_{1,t-1} + \gamma_{1,t}u_{1,t-1}) \\ D_t'(\rho_{2,t-1} + \gamma_{2,t}u_{2,t-1}) \end{bmatrix}$$

$$\begin{bmatrix} u_{1,t} \\ u_{2,t} \end{bmatrix} = \left\{ 1 + \tfrac{1}{\nu}(v_{1,t}, v_{2,t}) \left[\begin{pmatrix} \Omega^{-1}_{v,1,1} & 0 \\ \Omega^{-1}_{v,2,1} & \Omega^{-1}_{v,2,2} \end{pmatrix} \begin{pmatrix} \Omega^{-1}_{v,1,1} & \Omega^{-1}_{v,2,1} \\ 0 & \Omega^{-1}_{v,2,2} \end{pmatrix} \right]^{-1} \begin{pmatrix} v_{1,t} \\ v_{2,t} \end{pmatrix} \right\}^{-1} \begin{pmatrix} v_{1,t} \\ v_{2,t} \end{pmatrix}$$

Basic structural model:

$$\begin{bmatrix} \mu_{1,t} \\ \mu_{2,t} \end{bmatrix} = \begin{bmatrix} \Phi_{1,1} & \Phi_{1,2} \\ \Phi_{2,1} & \Phi_{2,2} \end{bmatrix} \begin{bmatrix} \mu_{1,t-1} \\ \mu_{2,t-1} \end{bmatrix} + \begin{bmatrix} \eta_{1,t} \\ \eta_{2,t} \end{bmatrix}$$

$$\begin{bmatrix} s_{1,t} \\ s_{2,t} \end{bmatrix} = \begin{bmatrix} D_t'\rho_{1,t} \\ D_t'\rho_{2,t} \end{bmatrix} = \begin{bmatrix} D_t'(\rho_{1,t-1} + \xi_{1,t}) \\ D_t'(\rho_{2,t-1} + \xi_{2,t}) \end{bmatrix}$$

'MDS' denotes the p-value of the martingale difference sequence test. Bold numbers indicate superior model performance. C_1 is the maximum modulus of eigenvalues of Φ. C_3 and C_4 are the maximum moduli of eigenvalues of $\hat{E}(X_t)$ and $\hat{E}(X_t \otimes X_t)$, respectively. We summarize ADF results for Conditions 2 to 4 and matrix Q_t, by using 'All stationary'. Standard errors are in parentheses. *, ** and *** indicate significance at the 5% and 1% levels, respectively.

Table 4
Parameter estimates and model diagnostics (Gaussian Seasonal-VARMA).

Seasonal-VARMA			
c_1	$-0.0122(0.0473)$	$\gamma_{2,\text{Jan}}$	$-0.0584^{***}(0.0094)$
c_2	$0.2549^{***}(0.0754)$	$\gamma_{2,\text{Feb}}$	$-0.0902^{***}(0.0185)$
$\Phi_{1,1}$	$0.6248^{***}(0.1031)$	$\gamma_{2,\text{Mar}}$	$-0.0056(0.0208)$
$\Phi_{1,2}$	$0.0484(0.0335)$	$\gamma_{2,\text{Apr}}$	$0.0431^{***}(0.0112)$
$\Phi_{2,1}$	$-0.7541^{***}(0.2900)$	$\gamma_{2,\text{May}}$	$0.0356(0.0359)$
$\Phi_{2,2}$	$0.3865^{***}(0.0647)$	$\gamma_{2,\text{Jun}}$	$0.0839^{***}(0.0094)$
$\Psi_{1,1}$	$-0.2706^{***}(0.0940)$	$\gamma_{2,\text{Jul}}$	$-0.0695^{***}(0.0087)$
$\Psi_{1,2}$	$0.0003(0.0171)$	$\gamma_{2,\text{Aug}}$	$-0.0318^{***}(0.0085)$
$\Psi_{2,1}$	$0.1361^{**}(0.0655)$	$\gamma_{2,\text{Sep}}$	$0.0319^{*}(0.0191)$
$\Psi_{2,2}$	$0.3169^{***}(0.0423)$	$\gamma_{2,\text{Oct}}$	$-0.0039(0.0145)$
$\Omega^{-1}_{v,1,1}$	$1.8231^{***}(0.0424)$	$\gamma_{2,\text{Nov}}$	$-0.0242(0.0257)$
$\Omega^{-1}_{v,2,1}$	$-0.3318^{***}(0.0537)$	$\gamma_{2,\text{Dec}}$	$0.1632^{***}(0.0296)$
$\Omega^{-1}_{v,2,2}$	$4.1728^{***}(0.1040)$	C_1	0.5272
$\gamma_{1,\text{Jan}}$	$-0.8857^{***}(0.0672)$	C_2	0.8398
$\gamma_{1,\text{Feb}}$	$0.1523(0.1702)$	MDS $v_{1,t}$	0.5582
$\gamma_{1,\text{Mar}}$	$0.3098^{**}(0.1216)$	MDS $v_{2,t}$	0.2126
$\gamma_{1,\text{Apr}}$	$0.0909(0.0777)$	LL	-4.8670
$\gamma_{1,\text{May}}$	$0.1898(0.1223)$	AIC	9.9111
$\gamma_{1,\text{Jun}}$	$0.1578^{**}(0.0732)$	BIC	10.2683
$\gamma_{1,\text{Jul}}$	$0.9664^{***}(0.1335)$	HQC	10.0523
$\gamma_{1,\text{Aug}}$	$0.2705^{***}(0.0999)$		
$\gamma_{1,\text{Sep}}$	$0.0219(0.1544)$		
$\gamma_{1,\text{Oct}}$	$0.6388^{***}(0.0905)$		
$\gamma_{1,\text{Nov}}$	$0.0520(0.1538)$		
$\gamma_{1,\text{Dec}}$	$-0.1005(0.1893)$		

For the model presented in this table, y_t is decomposed as

$$\begin{bmatrix} y_{1,t} \\ y_{2,t} \end{bmatrix} = \begin{bmatrix} c_1 \\ c_2 \end{bmatrix} + \begin{bmatrix} \mu_{1,t} \\ \mu_{2,t} \end{bmatrix} + \begin{bmatrix} s_{1,t} \\ s_{2,t} \end{bmatrix} + \begin{bmatrix} v_{1,t} \\ v_{2,t} \end{bmatrix}$$

$$\begin{bmatrix} \mu_{1,t} \\ \mu_{2,t} \end{bmatrix} = \begin{bmatrix} \Phi_{1,1} & \Phi_{1,2} \\ \Phi_{2,1} & \Phi_{2,2} \end{bmatrix} \begin{bmatrix} \mu_{1,t-1} \\ \mu_{2,t-1} \end{bmatrix} + \begin{bmatrix} \Psi_{1,1} & \Psi_{1,2} \\ \Psi_{2,1} & \Psi_{2,2} \end{bmatrix} \begin{bmatrix} v_{1,t-1} \\ v_{2,t-1} \end{bmatrix}$$

$$\begin{bmatrix} s_{1,t} \\ s_{2,t} \end{bmatrix} = \begin{bmatrix} D_t' \rho_{1,t} \\ D_t' \rho_{2,t} \end{bmatrix} = \begin{bmatrix} D_t'(\rho_{1,t-1} + \gamma_{1,t} v_{1,t-1}) \\ D_t'(\rho_{2,t-1} + \gamma_{2,t} v_{2,t-1}) \end{bmatrix}$$

A representation of Gaussian Seasonal-VARMA is presented in Equation (15). 'MDS' denotes the p-value of the martingale difference sequence test. C_1 and C_2 are the maximum moduli of eigenvalues of Φ and $\Psi - \Phi$, respectively. Standard errors are in parentheses. *, ** and *** indicate significance at the 10%, 5% and 1% levels, respectively.

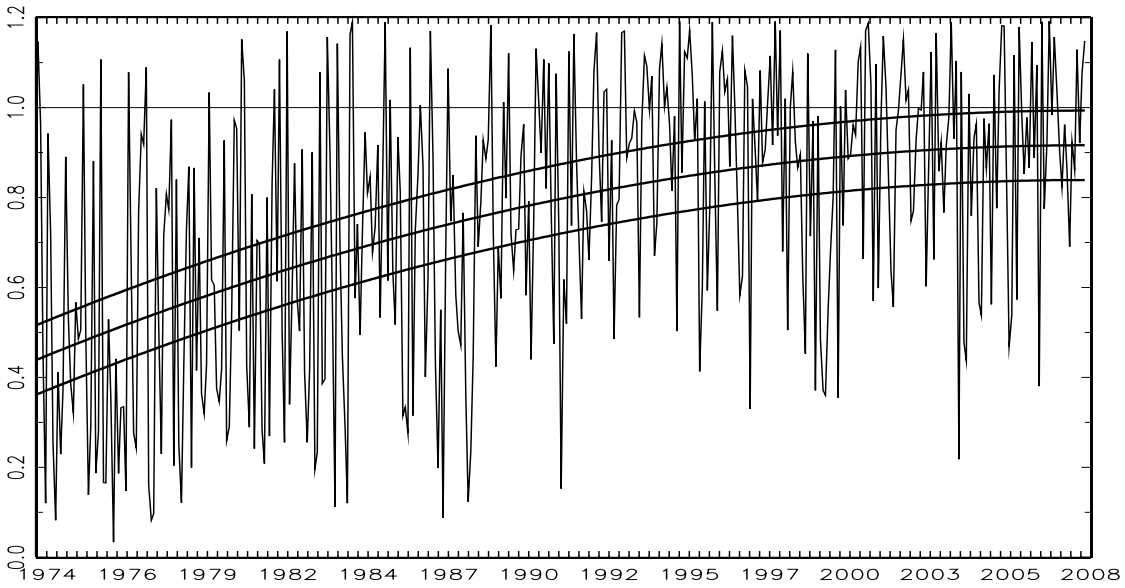

Fig. 2. Invertibility of Seasonal-QVAR (evolution of the maximum modulus of eigenvalues of Ψ_t for $t = 1, \ldots, T$). $\hat{\Psi}_t = 0.435881 + 0.002298t - 0.000003t^2$ and the 90% confidence interval are presented with thick lines. The value one is outside the confidence interval for all t.

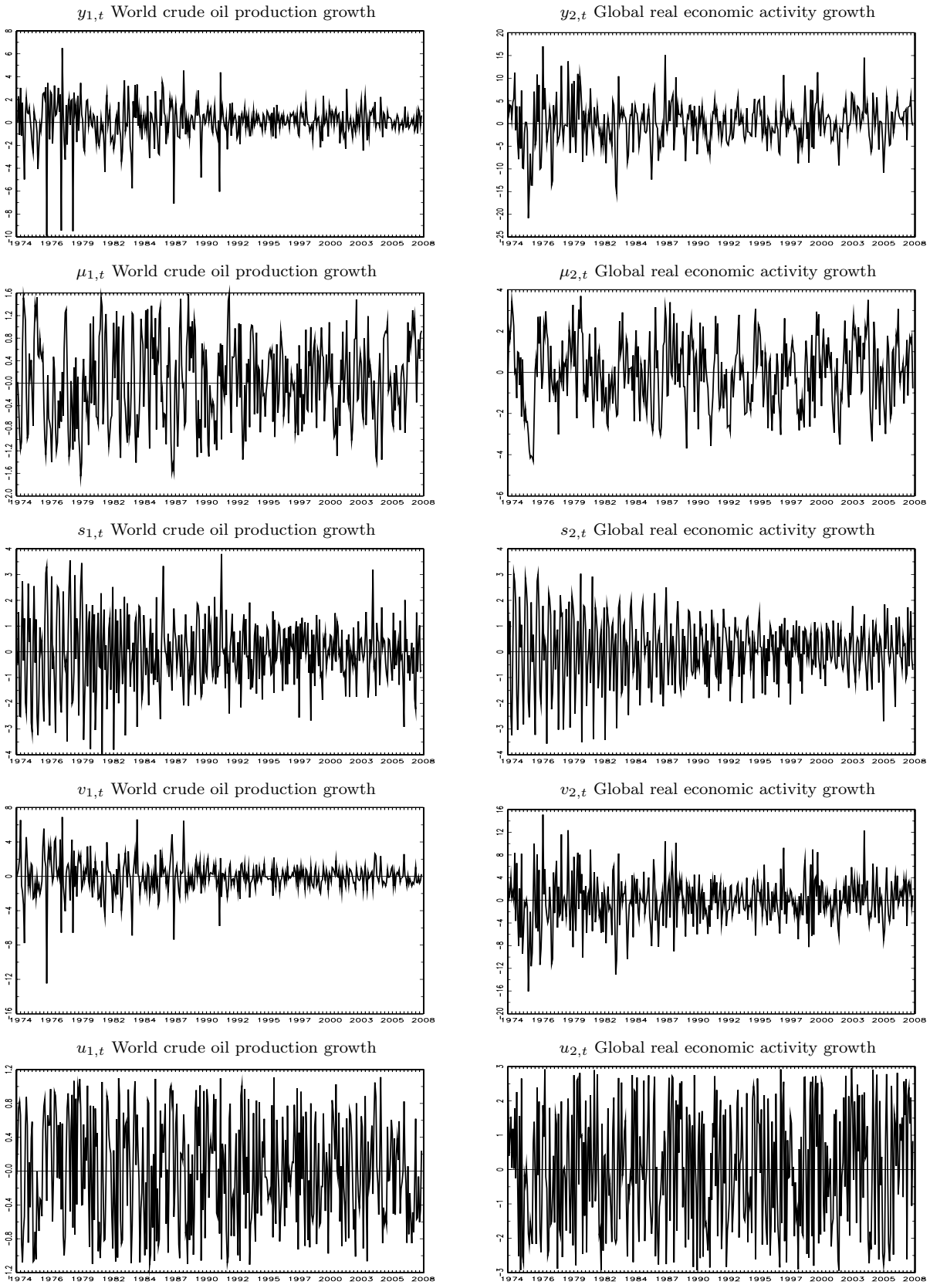

Fig. 3. Time series components of Seasonal-QVAR (March 1973 to December 2007).

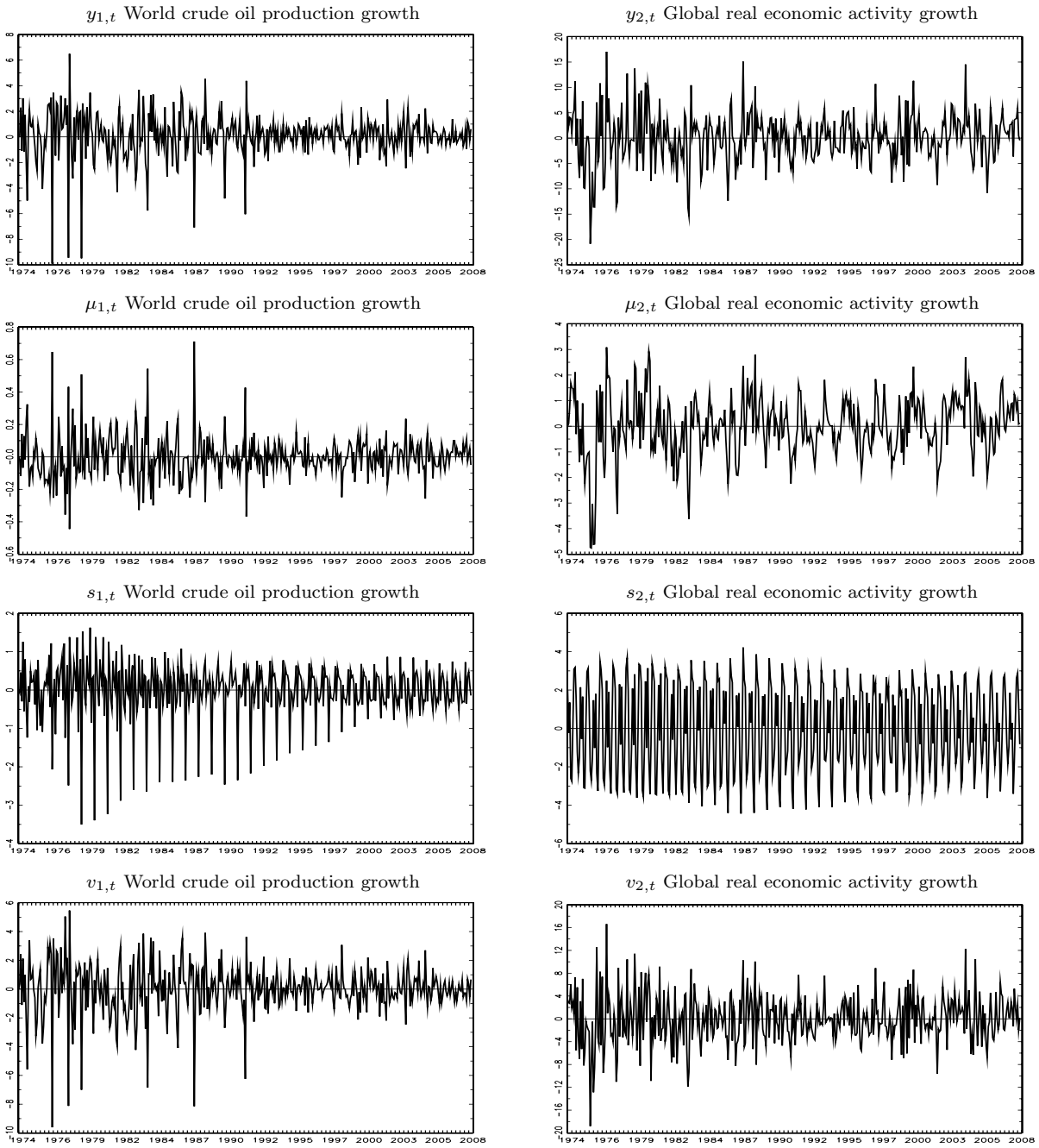

Fig. 4. Time series components of the basic structural model (March 1973 to December 2007).

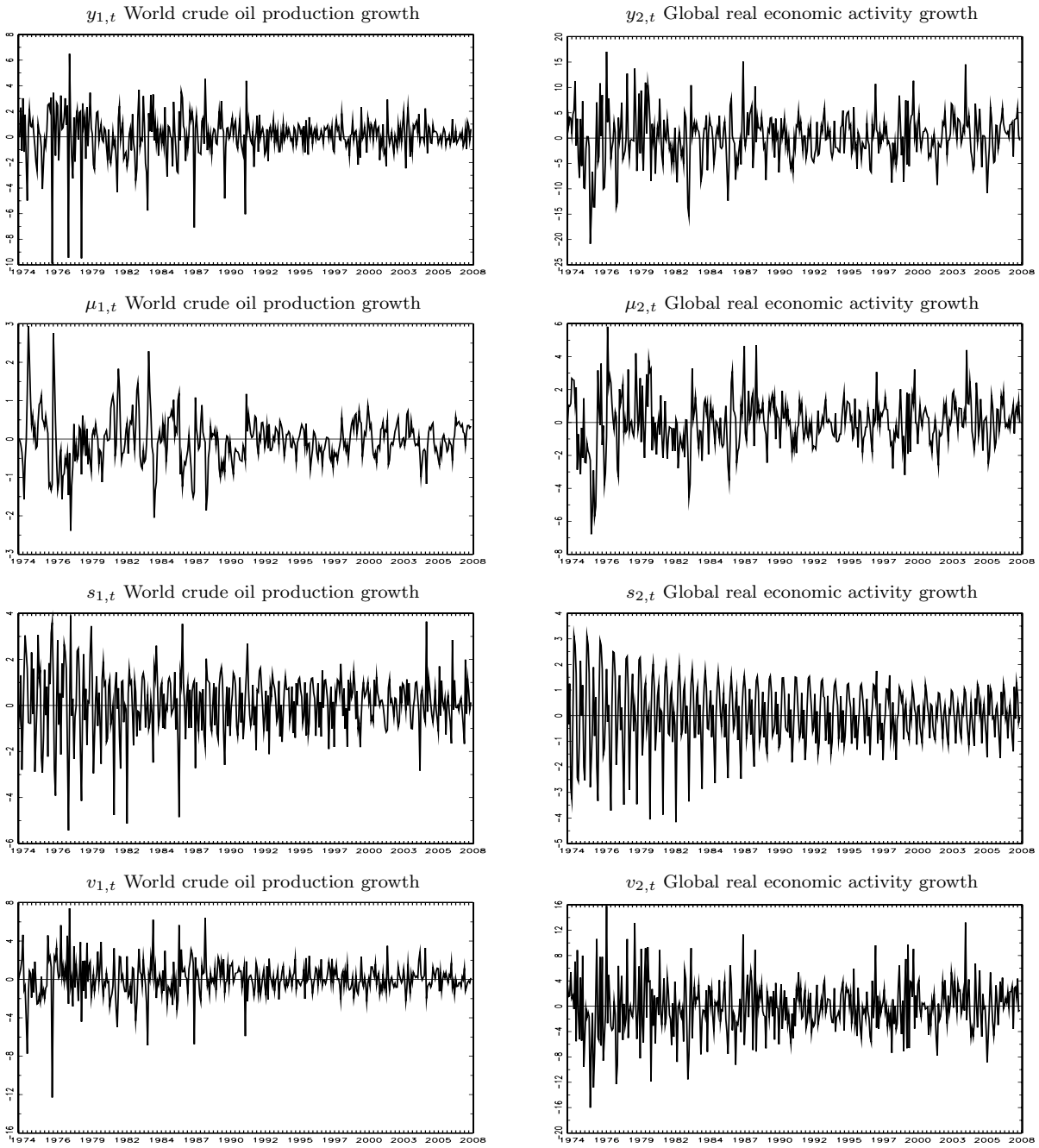

Fig. 5. Time series components of Gaussian Seasonal-VARMA (March 1973 to December 2007).

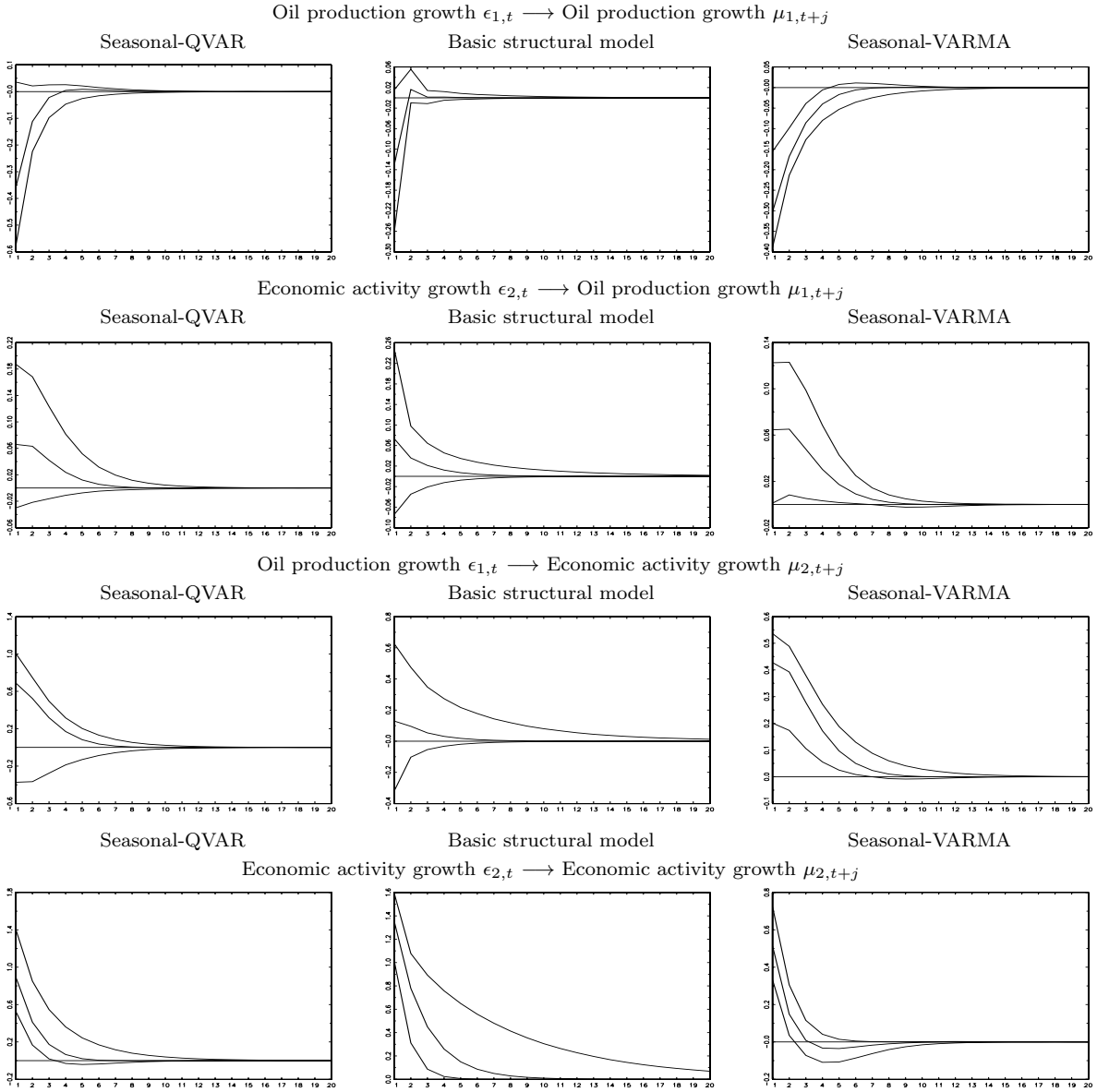

Fig. 6. Impulse response function with 90% confidence interval (Seasonal-QVAR; basic structural model; Seasonal-VARMA). The IRF confidence interval is estimated by using 10,000 Monte Carlo simulations from the ML estimates.

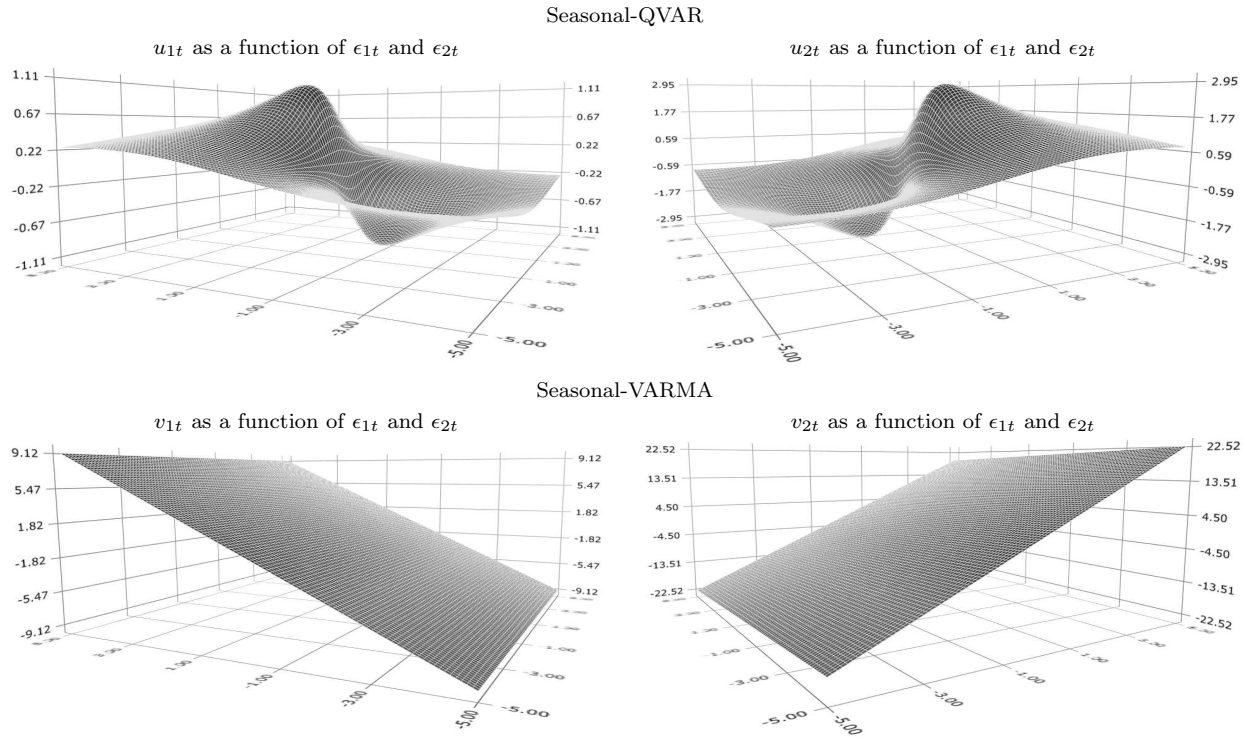

Fig. 7. Robustness to extreme values in the noise (Seasonal-QVAR; Seasonal-VARMA).

4. Application to crude oil production and industrial production

4.1. Motivation

Since the middle of the last century, the influence of the level of world aggregate oil production on the industrial production of different regions and countries have been analyzed in the economic literature. In this section we focus on this relation specifically for the United States and Canada, motivated by the following reasons:

First, Canada was the second largest commercial partner of the United States in 2017 (source: United States Census Bureau). The United States and Canada had a total trade of USD673.9 billion in 2017, which is the sum of USD341.2 billion of exports from the United States into Canada and USD332.8 billion of imports from Canada into the United States (source: Office of the United States Trade Representative). In 2017, Canada was the most important destination of the United States goods exports (USD282.5 billion, 18.3% of the total United States goods exports), and the third largest source of goods imported into the United States (USD300.0

billion, 12.8% of the total United States goods imports) (source: Office of the United States Trade Representative).

Second, both the United States and Canada are among the largest oil producers in the world. The United States was the third largest oil producer in 2016, and Canada was the ninth largest oil producer in the same year (source: United States Energy Information Administration). Mineral fuels, which include crude oil, are the largest category of imports into the United States from Canada (USD73 billion) in 2017 (source: Office of the United States Trade Representative). Furthermore, mineral fuels are the fourth largest category of exports of the United States into Canada (USD19 billion) in 2017, following vehicles, machinery and electrical machinery (source: Office of the United States Trade Representative).

Third, the United States started bilateral trade negotiations with Canada in 1986, resulting in the Canada-United States Free Trade Agreement (CUSFTA) that was brought into force on January 1, 1989 (source: Office of the United States Trade Representative). Presently, the commercial relation between the United States and Canada is regulated by the NAFTA, which was implemented on January 1, 1994 (source: Office of the United States Trade Representative). The current government of the United States argued that the treaty created problems for the United States economy, and it expressed its desire to renegotiate NAFTA (source: Office of the United States Trade Representative). As a consequence, NAFTA is being renegotiated (the seventh round of NAFTA negotiations were in March 2018).

Fourth, in this paper we extend the data period with respect to previous studies on the crude oil production and industrial production relation for different regions of the world (Nordhaus, Houthakker, and Sachs 1980; Kilian 2008; Peersman and Van Robays 2009; Baumeister and Peersman 2013; Kilian and Lütkepohl 2017), focusing on the United States and Canada.

4.2. Extended macroeconomic data

We use an extended macroeconomic dataset that covers the period of March 1973 to February 2018. We obtained monthly data on world crude oil production growth from Bloomberg for the period of January 2001 to February 2018 (ticker: DWOPWRLD Index; DOE World Crude Oil

Production Data). To validate the use of these data, we estimated the correlation coefficient between the world crude oil production growth variable from the classic dataset (i.e., from Kilian and Lütkepohl 2017; see Section 3.1) and the world crude oil production growth variable from Bloomberg. For the correlation analysis, we use the data period that is available from both sources (i.e., from January 2001 to December 2007; 83 observations from each variable). The estimated correlation coefficient is 0.9942, thus the two time series practically coincide for the period of 2001 to 2007. Motivated by this result, we extend the classic macroeconomic dataset of world crude oil production growth by using Bloomberg world crude oil production data.

We also use monthly data on the non-seasonally adjusted total industrial production growths of the United States and Canada (source: Organisation for Economic Co-operation and Development, OECD, https://data.oecd.org/industry/industrial-production.htm). We use total industrial production as an alternative to global real economic activity (Section 3), because global real economic activity is not available for the extended data period and because industrial production has a significant seasonality component. The use of the total industrial production variable is also motivated by the work of Kilian (2009). Descriptive statistics and ADF with constant test results are reported in Table 5.

Table 5
Descriptive statistics.

Descriptive statistics	World crude oil production growth	United States industrial production growth	Canada industrial production growth
Start date	March 1973	March 1973	March 1973
End date	February 2018	February 2018	February 2018
Sample size T	540	540	540
Minimum	−9.9073	−4.4296	−3.8376
Maximum	6.4986	2.0658	3.4561
Mean	0.0739	0.1545	0.1359
Standard deviation	1.5391	0.7177	1.0819
Skewness	−1.6380	−1.3244	−0.2575
Excess kurtosis	10.2169	6.1861	0.5930
ADF	−25.2821***	−8.23283***	−9.7543***

Growth in variables is measured in percentage points. *** indicates significance at the 1% level.

4.3. ML estimation results and model diagnostics

In this section, we report ML estimation results for the joint estimation of local level, seasonality and irregular components for the extended monthly macroeconomic dataset. We present results for three bivariate alternatives of variable selection. For the first alternative, we use the variables: world crude oil production growth $y_{1,t}$ and total industrial production growth of the United States $y_{2,t}$. For the second alternative, we use the variables: world crude oil production growth $y_{1,t}$ and total industrial production growth of Canada $y_{2,t}$. For the third alternative, we use the variables: total industrial production growth of the United States $y_{1,t}$ and total industrial production growth of Canada $y_{2,t}$. We estimate three bivariate models instead of one three-dimensional model, because the ML procedure does not converge to an optimum for a three-dimensional Seasonal-QVAR specification due to the relatively small sample size of the extended dataset. The bivariate Seasonal-QVAR estimates provide effective results about the dynamic interaction effects for the variables: world crude oil production growth, total industrial production growth of the United States, and total industrial production growth of Canada.

For each alternative of variable selection, we present the parameter estimates and model diagnostics of all models in Tables 6 to 8, respectively. For Seasonal-QVAR, we study the condition of invertibility in Fig. 8. For each alternative of variable selection, we present the time series components of Seasonal-QVAR in Figs. 9 to 11, respectively. We report the score function estimates for Seasonal-QVAR in Fig. 12.

Consistency and asymptotic normality of the ML estimates are supported by C_1, C_2, C_3 or C_4 for each model (Tables 6 to 8). For Seasonal-QVAR, the maximum modulus of eigenvalues of Ψ_t is lower than one for the three alternatives for variable selection (Fig. 8), supporting the invertibility of QVAR. We perform the Escanciano–Lobato (2009) MDS test for ϵ_t and u_t of Seasonal-QVAR, and we perform the same MDS test for v_t of the basic structural model and Seasonal-VARMA. For Seasonal-QVAR, MDS is rejected for one residual time series (Table 6), at the 10% level of significance. In all other cases of v_t and u_t, MDS is never rejected for Seasonal-QVAR (Tables 6 to 8). Furthermore, MDS is never rejected for the basic structural

model and for Seasonal-VARMA (Tables 6 to 8).

We compare statistical performances by using the LL, AIC, BIC and HQC metrics. All those metrics indicate an improvement in the model performance of Seasonal-QVAR, with respect to the basic structural model and Seasonal-VARMA (Tables 6 to 8). The estimates of $s_{1,t}$ and $s_{2,t}$ in Figs. 9 to 11 indicate significant seasonality effects with dynamic amplitude for all models, which support the use of stochastic seasonality. We also find that the local level estimates $\mu_{1,t}$ and $\mu_{2,t}$ are relatively homogeneous for Seasonal-QVAR, compared to the Gaussian alternatives (Figs. 9 to 11). This result is very similar to that one found for the classic macroeconomic dataset (Section 3), suggesting that extreme observations in many cases appear in the error term of Seasonal-QVAR, while extreme observations for some cases appear in the local level components of the basic structural model and Seasonal-VARMA. For the three alternatives of variable selection, the score function $u_t = (u_{1t}, u_{2t})'$ discounts extreme values from the structural-form error term $\epsilon_t = (\epsilon_{1t}, \epsilon_{2t})'$ for Seasonal-QVAR. In Fig. 12, we present each element of the updating vector $u_t = (u_{1t}, u_{2t})'$ of Seasonal-QVAR, as a function of ϵ_{1t} and ϵ_{2t} (those findings are similar to the ones reported in Fig. 7).

4.4. Dynamic interaction effects

In this section, we present the IRF estimates for each alternative of variable selection in Figs. 13 to 15, respectively. With respect to the interaction effects between world crude oil production growth $y_{1,t}$ and industrial production growth of the United States $y_{2,t}$, we present the IRF estimates with the 90% Monte Carlo confidence interval for Seasonal-QVAR, the basic structural model and Seasonal-VARMA in Fig. 13. The signs of the IRF estimates coincide for Seasonal-QVAR, the basic structural model and Seasonal-VARMA. We highlight in this figure the dynamic interaction effects: industrial production growth of the United States $\epsilon_{2,t}$ $\longrightarrow$ world crude oil production growth $\mu_{1,t+j}$. Those effects are about six times higher for the basic structural model and Seasonal-VARMA than for Seasonal-QVAR. Given the LL-based superiority of Seasonal-QVAR, the IRF estimates suggest that the basic structural model and Seasonal-VARMA overestimate the dynamic effects of the industrial production growth of the

United States on the world crude oil production growth variable. With respect to Fig. 13, it is noteworthy that the signs of all dynamic interaction effects coincide with those for the classic macroeconomic dataset (Fig. 6). The main difference between Figs. 6 and 13 is that the IRF estimates are more precise for the extended dataset than for the classic macroeconomic dataset, due to the higher sample size of the extended dataset.

With respect to the interaction effects between world crude oil production growth $y_{1,t}$ and industrial production growth of Canada $y_{2,t}$, we present the IRF estimates with the 90% Monte Carlo confidence interval for Seasonal-QVAR, the basic structural model and Seasonal-VARMA in Fig. 14. The signs of the IRF for the basic structural model and Seasonal-VARMA differ from the sign of IRF for Seasonal-QVAR. In Fig. 14, we highlight the dynamic interaction effects: world crude oil production growth $\epsilon_{1,t} \longrightarrow$ industrial production growth of Canada $\mu_{2,t+j}$. For Seasonal-QVAR significant positive interaction effects are measured, while for Seasonal-VARMA the opposite significant negative interaction effects are measured. Given the LL-based superiority of Seasonal-QVAR, the IRF suggests that the estimates of the dynamic effects of world crude oil production growth on industrial production growth of the Canada corresponding to Seasonal-VARMA are incorrect. Furthermore, the IRF estimates for the basic structural model are less precise than for Seasonal-QVAR, due to the wider Monte Carlo confidence intervals of the basic structural model.

With respect to the interaction effects between industrial production growth of the United States $y_{1,t}$ and industrial production growth of Canada $y_{2,t}$, we present the IRF estimates with the 90% Monte Carlo confidence interval for Seasonal-QVAR, the basic structural model and Seasonal-VARMA in Fig. 15. The IRF estimates are similar for the alternative models. We find that the IRF estimates for the basic structural model are less precise than for Seasonal-QVAR. For Seasonal-VARMA, the dynamic interaction effects between the industrial production growths of the United States and Canada are significantly positive in both directions. We repeat from point five of this section that world crude oil production growth has positive dynamic effects on the industrial production growth of the United States for Seasonal-VARMA (Fig. 13). This

result, combined with the positive interactions between the industrial production growths of the United States and Canada (Fig. 15), suggests that the negative interaction effects from world crude oil production growth to the industrial production growth of Canada estimated for Seasonal-VARMA (Fig. 14) are incorrect. This is due to the fact that the transitivity of the dynamic interaction effects among the three variables, world crude oil production growth, industrial production growth of the United States, and industrial production growth of Canada, fails for the IRF estimates of Seasonal-VARMA.

For the latter alternative of variable selection, we also estimate all models with the two variables: total industrial production growth of Canada $y_{1,t}$ and total industrial production growth of the United States $y_{2,t}$ (i.e., we use the opposite order of variables). We find the same results for likelihood-based performances, model diagnostics and dynamic interaction effects for both orders of variables. The related estimation results are available from the authors.

The IRF estimates (Figs. 13 to 15) combined with the LL-based model performance metrics (Tables 6 to 8) suggest that Seasonal-QVAR provides better IRF estimates than Seasonal-VARMA and the basic structural model. Seasonal-QVAR is robust to extreme observations (Fig. 12), and its ability to measure nonlinear dynamic interactions among variables creates a superior in-sample statistical performance with respect to the Gaussian multivariate time series models. These findings suggest the use of Seasonal-QVAR for the extended macroeconomic dataset, in order to study the macroeconomic question about the influence of world crude oil production growth on the industrial production growths of the United States and Canada.

Table 6

Parameter estimates and model diagnostics (variables: world crude oil production growth $y_{1,t}$ and total industrial production growth of the United States $y_{2,t}$).

Seasonal-QVAR				Basic structural model		Seasonal-VARMA			
c_1	0.1448***(0.0390)	$\gamma_{2,\text{Jan}}$	−0.0476(0.0451)	c_1	0.0758(0.2416)	c_1	0.0698(0.0428)	$\gamma_{2,\text{Jan}}$	−0.0084(0.0273)
c_2	0.1326***(0.0493)	$\gamma_{2,\text{Feb}}$	−0.0298(0.0669)	c_2	0.1517(0.2626)	c_2	0.1467***(0.0462)	$\gamma_{2,\text{Feb}}$	−0.0005(0.0184)
$\Phi_{1,1}$	0.5564***(0.0293)	$\gamma_{2,\text{Mar}}$	0.0094(0.0184)	$\Phi_{1,1}$	−0.1959*(0.1040)	$\Phi_{1,1}$	0.5818***(0.0737)	$\gamma_{2,\text{Mar}}$	0.0819(0.0741)
$\Phi_{1,2}$	0.1289***(0.0335)	$\gamma_{2,\text{Apr}}$	0.1009***(0.0341)	$\Phi_{1,2}$	0.3102(0.1975)	$\Phi_{1,2}$	0.3067***(0.1028)	$\gamma_{2,\text{Apr}}$	−0.0691*(0.0416)
$\Phi_{2,1}$	−0.3121***(0.0502)	$\gamma_{2,\text{May}}$	−0.3078***(0.0699)	$\Phi_{2,1}$	−0.2385(0.1612)	$\Phi_{2,1}$	−0.0886*(0.0520)	$\gamma_{2,\text{May}}$	0.0088(0.0137)
$\Phi_{2,2}$	0.9613***(0.0348)	$\gamma_{2,\text{Jun}}$	0.0540**(0.0265)	$\Phi_{2,2}$	0.8898***(0.0797)	$\Phi_{2,2}$	0.8227***(0.0496)	$\gamma_{2,\text{Jun}}$	0.0460*(0.0255)
$\Psi_{1,1}$	−0.1569***(0.0427)	$\gamma_{2,\text{Jul}}$	−0.2548***(0.0273)	$\Omega^{-1}_{v,1,1}$	0.7214*(0.4140)	$\Psi_{1,1}$	−0.2402***(0.0743)	$\gamma_{2,\text{Jul}}$	−0.3446***(0.1265)
$\Psi_{1,2}$	−0.0614**(0.0284)	$\gamma_{2,\text{Aug}}$	0.0287(0.0387)	$\Omega^{-1}_{v,2,1}$	−0.4278***(0.1085)	$\Psi_{1,2}$	0.0396(0.0715)	$\gamma_{2,\text{Aug}}$	0.1538(0.1314)
$\Psi_{2,1}$	0.0432(0.0304)	$\gamma_{2,\text{Sep}}$	0.0046(0.0436)	$\Omega^{-1}_{v,2,2}$	0.0000(0.0002)	$\Psi_{2,1}$	0.0029(0.0180)	$\gamma_{2,\text{Sep}}$	−0.1272**(0.0625)
$\Psi_{2,2}$	0.3979***(0.0437)	$\gamma_{2,\text{Oct}}$	0.0217(0.0311)	$\Omega^{-1}_{\eta,1,1}$	1.2482***(0.2349)	$\Psi_{2,2}$	0.2811***(0.0335)	$\gamma_{2,\text{Oct}}$	−0.0143(0.0262)
$\Omega^{-1}_{v,1,1}$	0.9347***(0.0268)	$\gamma_{2,\text{Nov}}$	−0.0552*(0.0318)	$\Omega^{-1}_{\eta,2,1}$	0.3410**(0.1434)	$\Omega^{-1}_{v,1,1}$	1.4160***(0.0423)	$\gamma_{2,\text{Nov}}$	0.0762(0.0848)
$\Omega^{-1}_{v,2,1}$	0.0585**(0.0237)	$\gamma_{2,\text{Dec}}$	0.1366***(0.0331)	$\Omega^{-1}_{\eta,2,2}$	0.2561***(0.0360)	$\Omega^{-1}_{v,2,1}$	0.1045***(0.0257)	$\gamma_{2,\text{Dec}}$	0.1443***(0.0445)
$\Omega^{-1}_{v,2,2}$	0.4523***(0.0123)	C_1	0.7860	$\sigma_{\xi,1}$	0.0350***(0.0096)	$\Omega^{-1}_{v,2,2}$	0.6313***(0.0180)	C_1	0.7112
ν	3.4886***(0.0611)	C_2 to C_4 ADF	All stationary	$\sigma_{\xi,2}$	0.0000(0.0034)	$\gamma_{1,\text{Jan}}$	−0.7343***(0.1536)	C_2	0.6853
$\gamma_{1,\text{Jan}}$	−0.2967***(0.0276)	C_3	0.8322	C_1	0.8167	$\gamma_{1,\text{Feb}}$	−0.0962(0.1210)	MDS $v_{1,t}$	0.6438
$\gamma_{1,\text{Feb}}$	0.1261***(0.0433)	C_4	0.7425	MDS $v_{1,t}$	0.8822	$\gamma_{1,\text{Mar}}$	0.2391**(0.1117)	MDS $v_{2,t}$	0.4723
$\gamma_{1,\text{Mar}}$	0.4312***(0.0427)	Q_t ADF	All stationary	MDS $v_{2,t}$	0.8747	$\gamma_{1,\text{Apr}}$	0.3026*(0.1631)	LL	−2.7257
$\gamma_{1,\text{Apr}}$	0.0299(0.0541)	MDS $v_{1,t}$	0.2602	LL	−2.8544	$\gamma_{1,\text{May}}$	0.2989***(0.1120)	AIC	5.5885
$\gamma_{1,\text{May}}$	0.4302***(0.0963)	MDS $v_{2,t}$	0.0601	AIC	5.7607	$\gamma_{1,\text{Jun}}$	0.4804***(0.1346)	BIC	5.8826
$\gamma_{1,\text{Jun}}$	0.6332***(0.0295)	MDS $u_{1,t}$	0.7141	BIC	5.8720	$\gamma_{1,\text{Jul}}$	−0.1665(0.1213)	HQC	5.7035
$\gamma_{1,\text{Jul}}$	−0.8235***(0.0273)	MDS $u_{2,t}$	0.5900	HQC	5.8042	$\gamma_{1,\text{Aug}}$	0.4066***(0.1262)		
$\gamma_{1,\text{Aug}}$	0.1553(0.1560)	LL	**−2.5503**			$\gamma_{1,\text{Sep}}$	−0.1456(0.1518)		
$\gamma_{1,\text{Sep}}$	−0.2243***(0.0802)	AIC	**5.2413**			$\gamma_{1,\text{Oct}}$	0.1401(0.1337)		
$\gamma_{1,\text{Oct}}$	0.6420***(0.0565)	BIC	**5.5433**			$\gamma_{1,\text{Nov}}$	0.0417(0.1160)		
$\gamma_{1,\text{Nov}}$	0.4841***(0.0524)	HQC	**5.3594**			$\gamma_{1,\text{Dec}}$	−0.1260(0.1567)		
$\gamma_{1,\text{Dec}}$	−0.1551*(0.0812)								

'MDS' denotes the p-value of the martingale difference sequence test. Bold numbers indicate superior model performance. Standard errors are in parentheses. *, ** and *** indicate significance at the 10%, 5% and 1% levels, respectively.

Table 7

Parameter estimates and model diagnostics (variables: world crude oil production growth $y_{1,t}$ and total industrial production growth of Canada $y_{2,t}$).

Seasonal-QVAR				Basic structural model		Seasonal-VARMA			
c_1	0.1621***(0.0243)	$\gamma_{2,\text{Jan}}$	−0.2320***(0.0247)	c_1	0.0773(0.2346)	c_1	0.0371(0.0255)	$\gamma_{2,\text{Jan}}$	0.0052(0.0131)
c_2	0.0948***(0.0242)	$\gamma_{2,\text{Feb}}$	−0.0028(0.0220)	c_2	0.1790(0.2499)	c_2	0.0945***(0.0230)	$\gamma_{2,\text{Feb}}$	0.0393(0.0274)
$\Phi_{1,1}$	4.0807***(0.0253)	$\gamma_{2,\text{Mar}}$	−0.0951***(0.0264)	$\Phi_{1,1}$	−0.0747*(0.0404)	$\Phi_{1,1}$	4.1131***(0.0305)	$\gamma_{2,\text{Mar}}$	0.0222(0.0252)
$\Phi_{1,2}$	−0.3984***(0.0042)	$\gamma_{2,\text{Apr}}$	−0.1323***(0.0271)	$\Phi_{1,2}$	0.0250(0.0588)	$\Phi_{1,2}$	−3.6588***(0.0255)	$\gamma_{2,\text{Apr}}$	0.0434(0.0321)
$\Phi_{2,1}$	33.7759***(0.0282)	$\gamma_{2,\text{May}}$	0.0637***(0.0240)	$\Phi_{2,1}$	0.0575*(0.0301)	$\Phi_{2,1}$	3.4918***(0.0233)	$\gamma_{2,\text{May}}$	−0.0250(0.0170)
$\Phi_{2,2}$	−3.2777***(0.0243)	$\gamma_{2,\text{Jun}}$	−0.2192***(0.0252)	$\Phi_{2,2}$	−0.0474(0.0419)	$\Phi_{2,2}$	−3.0287***(0.0318)	$\gamma_{2,\text{Jun}}$	0.0452(0.0298)
$\Psi_{1,1}$	0.0196***(0.0019)	$\gamma_{2,\text{Jul}}$	0.1629***(0.0274)	$\Omega^{-1}_{v,1,1}$	0.0000(0.0000)	$\Psi_{1,1}$	0.0363**(0.0168)	$\gamma_{2,\text{Jul}}$	0.2047***(0.0251)
$\Psi_{1,2}$	−0.0108***(0.0020)	$\gamma_{2,\text{Aug}}$	0.0223(0.0193)	$\Omega^{-1}_{v,2,1}$	0.0004(1.1289)	$\Psi_{1,2}$	−0.0549***(0.0177)	$\gamma_{2,\text{Aug}}$	0.0084(0.0254)
$\Psi_{2,1}$	0.1510***(0.0117)	$\gamma_{2,\text{Sep}}$	−0.0501**(0.0235)	$\Omega^{-1}_{v,2,2}$	0.0021(0.8367)	$\Psi_{2,1}$	0.0494***(0.0175)	$\gamma_{2,\text{Sep}}$	−0.0424(0.0310)
$\Psi_{2,2}$	−0.1762***(0.0109)	$\gamma_{2,\text{Oct}}$	0.1016***(0.0248)	$\Omega^{-1}_{\eta,1,1}$	1.4490***(0.0434)	$\Psi_{2,2}$	−0.0924***(0.0189)	$\gamma_{2,\text{Oct}}$	0.1105**(0.0459)
$\Omega^{-1}_{v,1,1}$	1.0080***(0.0138)	$\gamma_{2,\text{Nov}}$	−0.0617**(0.0296)	$\Omega^{-1}_{\eta,2,1}$	0.0832*(0.0475)	$\Omega^{-1}_{v,1,1}$	1.4317***(0.0343)	$\gamma_{2,\text{Nov}}$	−0.0181(0.0258)
$\Omega^{-1}_{v,2,1}$	0.0636***(0.0243)	$\gamma_{2,\text{Dec}}$	0.0901***(0.0239)	$\Omega^{-1}_{\eta,2,2}$	1.0826***(0.0412)	$\Omega^{-1}_{v,2,1}$	0.0216(0.0241)	$\gamma_{2,\text{Dec}}$	−0.0284(0.0286)
$\Omega^{-1}_{v,2,2}$	0.8861***(0.0221)	C_1	0.6853	$\sigma_{\xi,1}$	0.0357***(0.0098)	$\Omega^{-1}_{v,2,2}$	1.0501***(0.0251)	C_1	0.5642
ν	4.9868***(0.0738)	C_2 to C_4 ADF	All stationary	$\sigma_{\xi,2}$	0.0000(0.0000)	$\gamma_{1,\text{Jan}}$	−0.9794***(0.0340)	C_2	0.6598
$\gamma_{1,\text{Jan}}$	0.0035(0.0227)	C_3	0.6845	C_1	0.1014	$\gamma_{1,\text{Feb}}$	−0.3295***(0.0250)	MDS $v_{1,t}$	0.5488
$\gamma_{1,\text{Feb}}$	0.0140(0.0255)	C_4	0.4744	MDS $v_{1,t}$	0.8705	$\gamma_{1,\text{Mar}}$	−0.0735**(0.0296)	MDS $v_{2,t}$	0.8531
$\gamma_{1,\text{Mar}}$	0.5015***(0.0243)	Q_t ADF	All stationary	MDS $v_{2,t}$	0.8688	$\gamma_{1,\text{Apr}}$	−0.0336(0.0343)	LL	−3.2457
$\gamma_{1,\text{Apr}}$	−0.1559***(0.0244)	MDS $v_{1,t}$	0.1726	LL	−3.3615	$\gamma_{1,\text{May}}$	0.0765***(0.0251)	AIC	6.6284
$\gamma_{1,\text{May}}$	0.2402***(0.0243)	MDS $v_{2,t}$	0.9158	AIC	6.7748	$\gamma_{1,\text{Jun}}$	0.2956***(0.1018)	BIC	6.9225
$\gamma_{1,\text{Jun}}$	0.2865***(0.0243)	MDS $u_{1,t}$	0.7124	BIC	6.8861	$\gamma_{1,\text{Jul}}$	−0.4387***(0.0416)	HQC	6.7434
$\gamma_{1,\text{Jul}}$	−0.5107***(0.0244)	MDS $u_{2,t}$	0.9570	HQC	6.8184	$\gamma_{1,\text{Aug}}$	0.2774***(0.0595)		
$\gamma_{1,\text{Aug}}$	0.2376***(0.0244)	LL	**−3.1260**			$\gamma_{1,\text{Sep}}$	−0.3946***(0.0245)		
$\gamma_{1,\text{Sep}}$	−0.3173***(0.0244)	AIC	**6.3926**			$\gamma_{1,\text{Oct}}$	−0.0806(0.0515)		
$\gamma_{1,\text{Oct}}$	0.3719***(0.0243)	BIC	**6.6946**			$\gamma_{1,\text{Nov}}$	−0.3101***(0.0286)		
$\gamma_{1,\text{Nov}}$	0.0038(0.0278)	HQC	**6.5107**			$\gamma_{1,\text{Dec}}$	−0.4799***(0.0298)		
$\gamma_{1,\text{Dec}}$	0.3857***(0.0244)								

'MDS' denotes the p-value of the martingale difference sequence test. Bold numbers indicate superior model performance. Standard errors are in parentheses. *, ** and *** indicate significance at the 10%, 5% and 1% levels, respectively.

Table 8

Parameter estimates and model diagnostics (variables: total industrial production growths of the United States and Canada, $y_{1,t}$ and $y_{2,t}$, respectively).

Seasonal-QVAR				Basic structural model		Seasonal-VARMA			
c_1	0.1892***(0.0579)	$\gamma_{2,\text{Jan}}$	−0.0605*(0.0311)	c_1	0.1475(0.2701)	c_1	0.0974*(0.0497)	$\gamma_{2,\text{Jan}}$	−0.0339*(0.0190)
c_2	0.1850***(0.0559)	$\gamma_{2,\text{Feb}}$	0.0306(0.0197)	c_2	0.1780(0.2794)	c_2	0.0185(0.0408)	$\gamma_{2,\text{Feb}}$	0.0088(0.0102)
$\Phi_{1,1}$	0.7666***(0.1156)	$\gamma_{2,\text{Mar}}$	−0.0754(0.1320)	$\Phi_{1,1}$	0.7659***(0.0913)	$\Phi_{1,1}$	0.7312***(0.0639)	$\gamma_{2,\text{Mar}}$	−0.0005(0.0172)
$\Phi_{1,2}$	0.0568(0.0972)	$\gamma_{2,\text{Apr}}$	0.0369(0.0340)	$\Phi_{1,2}$	0.0674(0.0844)	$\Phi_{1,2}$	0.0513(0.0640)	$\gamma_{2,\text{Apr}}$	0.0046(0.0131)
$\Phi_{2,1}$	1.0012***(0.2095)	$\gamma_{2,\text{May}}$	−0.0762(0.0515)	$\Phi_{2,1}$	1.0513***(0.1896)	$\Phi_{2,1}$	0.9173***(0.1236)	$\gamma_{2,\text{May}}$	0.0430(0.0380)
$\Phi_{2,2}$	0.0408(0.1688)	$\gamma_{2,\text{Jun}}$	−0.0136(0.0385)	$\Phi_{2,2}$	−0.2117**(0.1011)	$\Phi_{2,2}$	−0.0070(0.1234)	$\gamma_{2,\text{Jun}}$	−0.0123(0.0227)
$\Psi_{1,1}$	0.3104***(0.0749)	$\gamma_{2,\text{Jul}}$	0.0008(0.0282)	$\Omega_{v,1,1}^{-1}$	0.5370***(0.0363)	$\Psi_{1,1}$	0.2617***(0.0479)	$\gamma_{2,\text{Jul}}$	0.0417(0.0565)
$\Psi_{1,2}$	0.1051***(0.0337)	$\gamma_{2,\text{Aug}}$	−0.0300(0.0253)	$\Omega_{v,2,1}^{-1}$	0.2369*(0.1427)	$\Psi_{1,2}$	0.0903***(0.0255)	$\gamma_{2,\text{Aug}}$	−0.0611(0.0397)
$\Psi_{2,1}$	0.4750***(0.1154)	$\gamma_{2,\text{Sep}}$	−0.0862***(0.0296)	$\Omega_{v,2,2}^{-1}$	0.0008(0.0311)	$\Psi_{2,1}$	0.3741***(0.0620)	$\gamma_{2,\text{Sep}}$	−0.0610***(0.0192)
$\Psi_{2,2}$	−0.2127***(0.0597)	$\gamma_{2,\text{Oct}}$	−0.1992***(0.0748)	$\Omega_{\eta,1,1}^{-1}$	0.2697***(0.0497)	$\Psi_{2,2}$	−0.2281***(0.0420)	$\gamma_{2,\text{Oct}}$	0.0482***(0.0157)
$\Omega_{v,1,1}^{-1}$	0.5480***(0.0257)	$\gamma_{2,\text{Nov}}$	0.0069(0.0114)	$\Omega_{\eta,2,1}^{-1}$	0.1002(0.2875)	$\Omega_{v,1,1}^{-1}$	0.6118***(0.0163)	$\gamma_{2,\text{Nov}}$	−0.1115(0.0688)
$\Omega_{v,2,1}^{-1}$	0.3122***(0.0378)	$\gamma_{2,\text{Dec}}$	0.0443(0.0621)	$\Omega_{\eta,2,2}^{-1}$	0.9459***(0.0341)	$\Omega_{v,2,1}^{-1}$	0.3307***(0.0395)	$\gamma_{2,\text{Dec}}$	0.2296***(0.0763)
$\Omega_{v,2,2}^{-1}$	0.8809***(0.0326)	C_1	0.8380	$\sigma_{\xi,1}$	0.0000(0.0007)	$\Omega_{v,2,2}^{-1}$	0.9452***(0.0285)	C_1	0.7903
ν	12.0833***(4.1508)	C_2 to C_4 ADF	All stationary	$\sigma_{\xi,2}$	0.0001(0.0004)	$\gamma_{1,\text{Jan}}$	0.1054(0.0930)	C_2	0.3536
$\gamma_{1,\text{Jan}}$	0.0973(0.2270)	C_3	0.8624	C_1	0.8337	$\gamma_{1,\text{Feb}}$	−0.5215***(0.0816)	MDS $v_{1,t}$	0.8441
$\gamma_{1,\text{Feb}}$	−0.4442***(0.1550)	C_4	0.7469	MDS $v_{1,t}$	0.9094	$\gamma_{1,\text{Mar}}$	−0.0721(0.0924)	MDS $v_{2,t}$	0.8881
$\gamma_{1,\text{Mar}}$	−0.0668(0.1761)	Q_t ADF	All stationary	MDS $v_{2,t}$	0.2975	$\gamma_{1,\text{Apr}}$	0.0829(0.0929)	LL	−2.2902
$\gamma_{1,\text{Apr}}$	−0.0587(0.1940)	MDS $v_{1,t}$	0.1788	LL	−2.4360	$\gamma_{1,\text{May}}$	0.0518(0.0891)	AIC	4.7174
$\gamma_{1,\text{May}}$	−0.0966(0.1461)	MDS $v_{2,t}$	0.6062	AIC	4.9238	$\gamma_{1,\text{Jun}}$	0.0226(0.0943)	BIC	5.0114
$\gamma_{1,\text{Jun}}$	−0.0274(0.1460)	MDS $u_{1,t}$	0.9892	BIC	5.0350	$\gamma_{1,\text{Jul}}$	−0.1978(0.1807)	HQC	4.8324
$\gamma_{1,\text{Jul}}$	−0.0796(0.2426)	MDS $u_{2,t}$	0.8381	HQC	4.9673	$\gamma_{1,\text{Aug}}$	−0.1790**(0.0698)		
$\gamma_{1,\text{Aug}}$	−0.1812(0.1705)	LL	**−2.2751**			$\gamma_{1,\text{Sep}}$	0.0880(0.0887)		
$\gamma_{1,\text{Sep}}$	−0.1227(0.1782)	AIC	**4.6909**			$\gamma_{1,\text{Oct}}$	−0.4465***(0.0840)		
$\gamma_{1,\text{Oct}}$	−0.7607***(0.2244)	BIC	**4.9929**			$\gamma_{1,\text{Nov}}$	0.0966(0.0872)		
$\gamma_{1,\text{Nov}}$	0.1743(0.1630)	HQC	**4.8090**			$\gamma_{1,\text{Dec}}$	0.5727***(0.0914)		
$\gamma_{1,\text{Dec}}$	0.5596***(0.2169)								

'MDS' denotes the p-value of the martingale difference sequence test. Bold numbers indicate superior model performance. Standard errors are in parentheses. *, ** and *** indicate significance at the 10%, 5% and 1% levels, respectively.

Variables: world crude oil production growth $y_{1,t}$ and total industrial production growth of the United States $y_{2,t}$

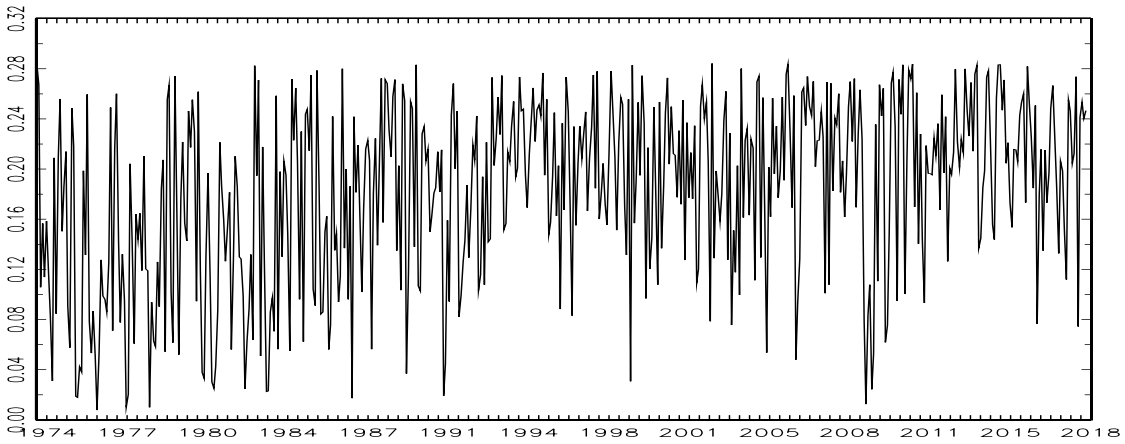

Variables: world crude oil production growth $y_{1,t}$ and total industrial production growth of Canada $y_{2,t}$

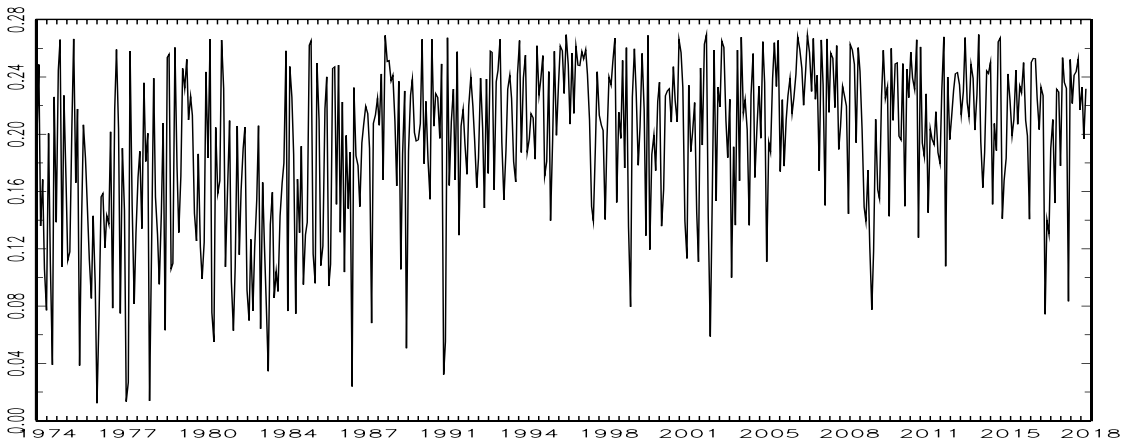

Variables: total industrial production growth of the United States $y_{1,t}$ and total industrial production growth of Canada $y_{2,t}$

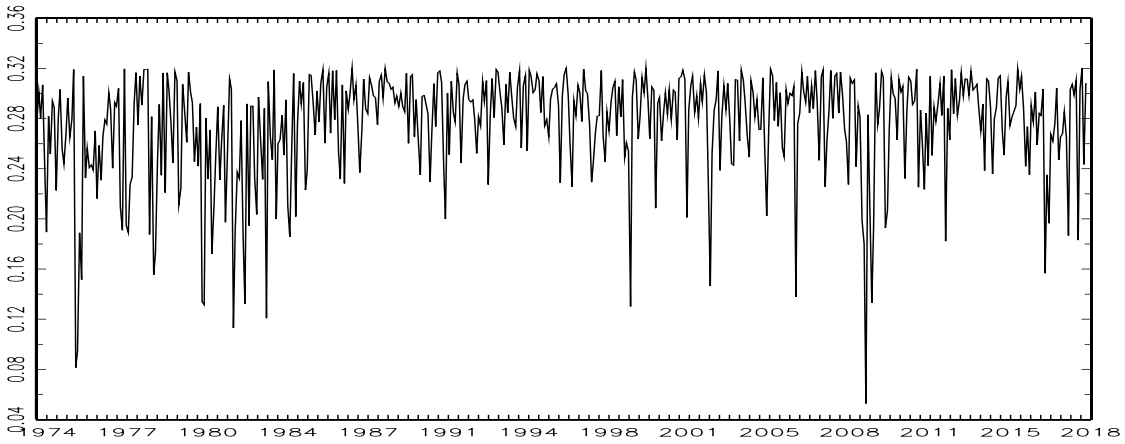

Fig. 8. Invertibility of Seasonal-QVAR (evolution of the maximum modulus of eigenvalues of Ψ_t for $t = 1, \ldots, T$).

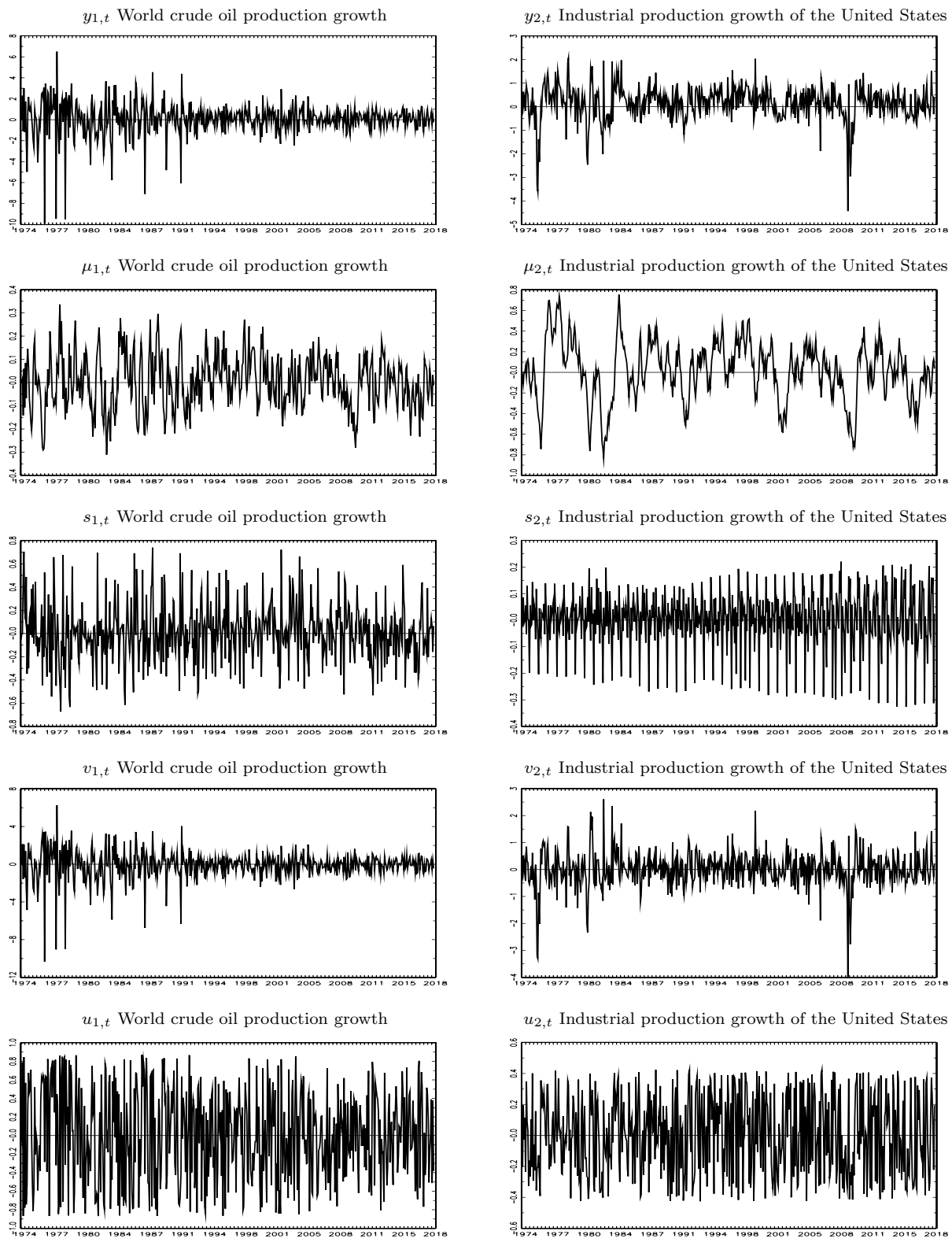

Fig. 9. Time series components of Seasonal-QVAR for the variables: world crude oil production growth $y_{1,t}$ and total industrial production growth of the United States $y_{2,t}$ (March 1973 to February 2018).

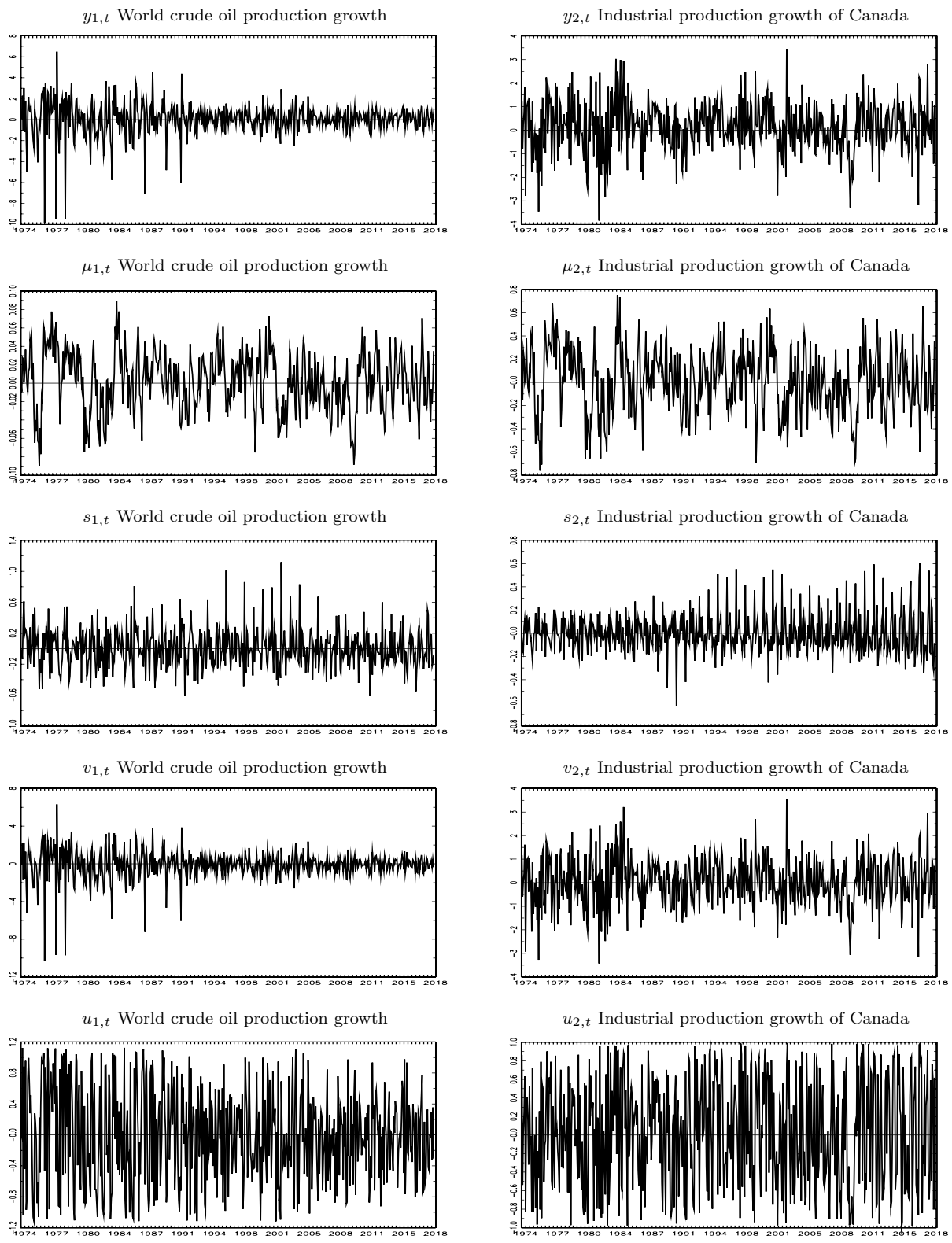

Fig. 10. Time series components of Seasonal-QVAR for the variables: world crude oil production growth $y_{1,t}$ and total industrial production growth of Canada $y_{2,t}$ (March 1973 to February 2018).

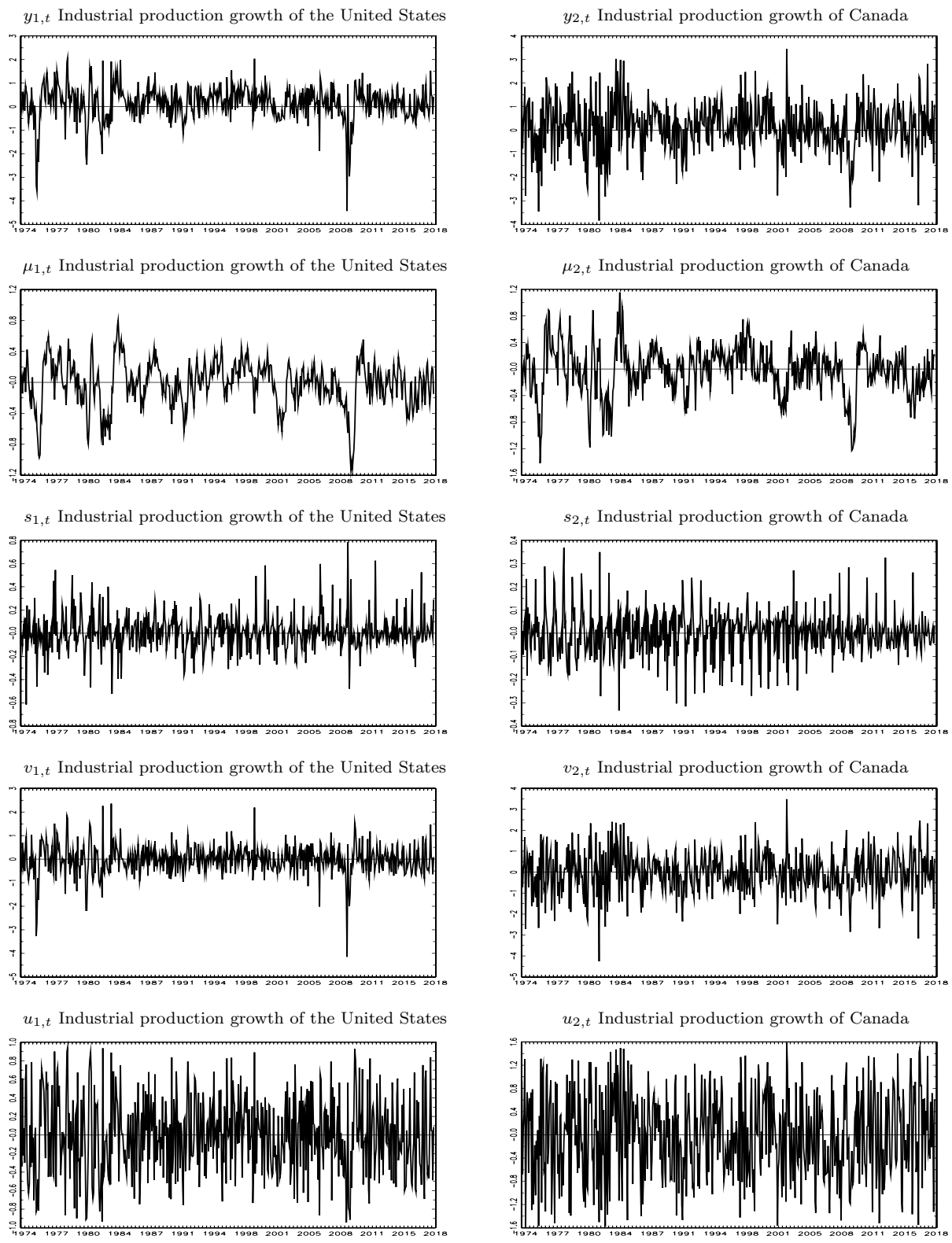

Fig. 11. Time series components of Seasonal-QVAR for the variables: total industrial production growth of the United States $y_{1,t}$ and total industrial production growth of Canada $y_{2,t}$ (March 1973 to February 2018).

Variables: world crude oil production growth $y_{1,t}$ and total industrial production growth of the United States $y_{2,t}$

u_{1t} as a function of ϵ_{1t} and ϵ_{2t}

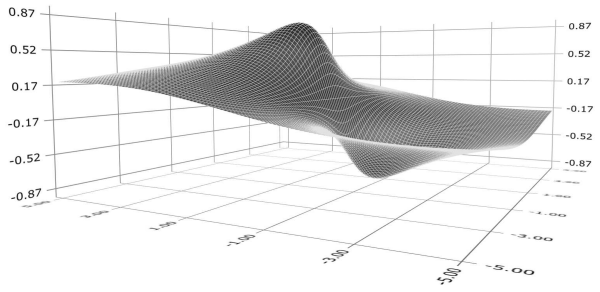

u_{2t} as a function of ϵ_{1t} and ϵ_{2t}

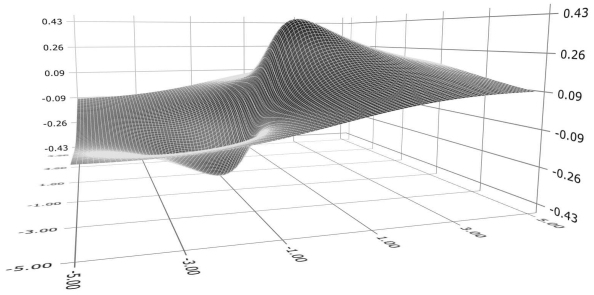

Variables: world crude oil production growth $y_{1,t}$ and total industrial production growth of Canada $y_{2,t}$

u_{1t} as a function of ϵ_{1t} and ϵ_{2t}

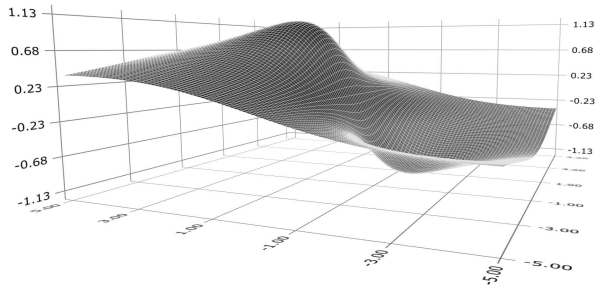

u_{2t} as a function of ϵ_{1t} and ϵ_{2t}

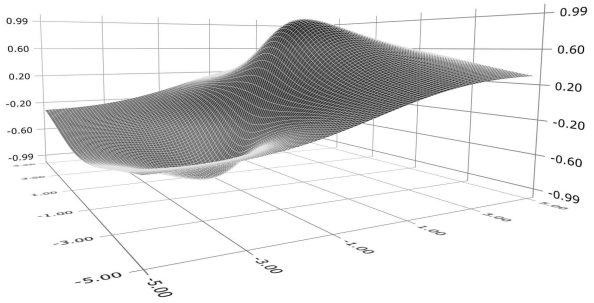

Variables: total industrial production growth of the United States $y_{1,t}$ and total industrial production growth of Canada $y_{2,t}$

u_{1t} as a function of ϵ_{1t} and ϵ_{2t}

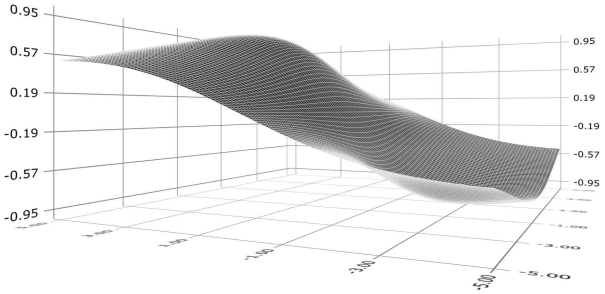

u_{2t} as a function of ϵ_{1t} and ϵ_{2t}

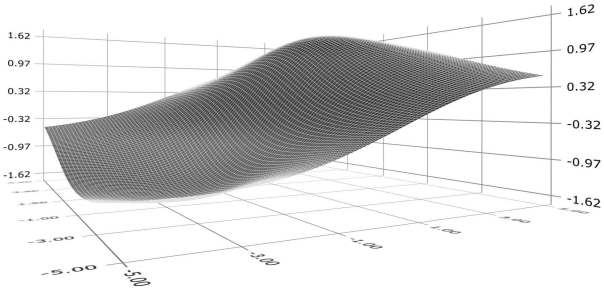

Fig. 12. Robustness to extreme values in the noise (Seasonal-QVAR).

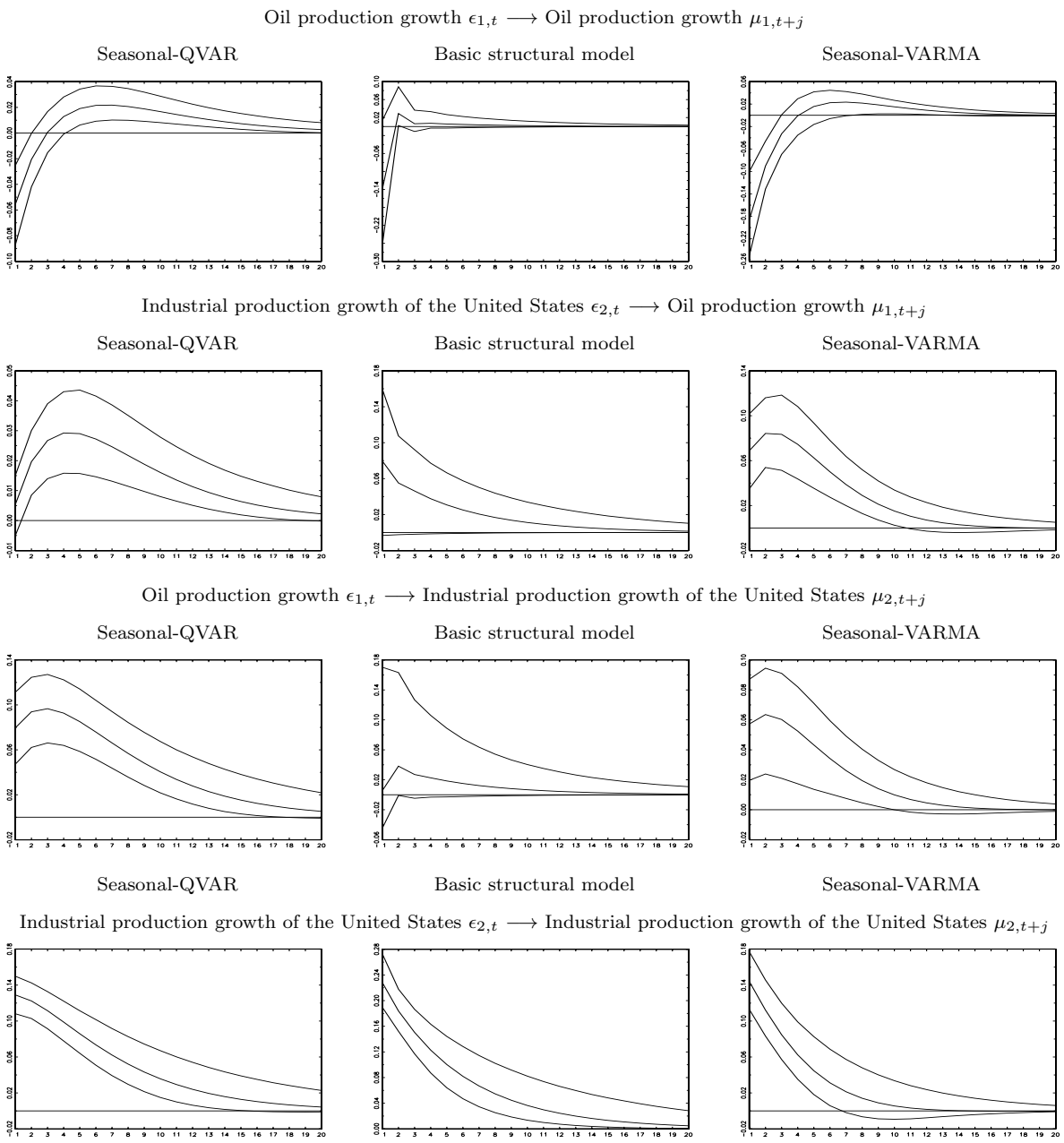

Fig. 13. Impulse response function with 90% confidence interval for the variables: world crude oil production growth $y_{1,t}$ and total industrial production growth of the United States $y_{2,t}$ (Seasonal-QVAR; basic structural model; Seasonal-VARMA). The IRF confidence interval is estimated by using 10,000 Monte Carlo simulations from the ML estimates.

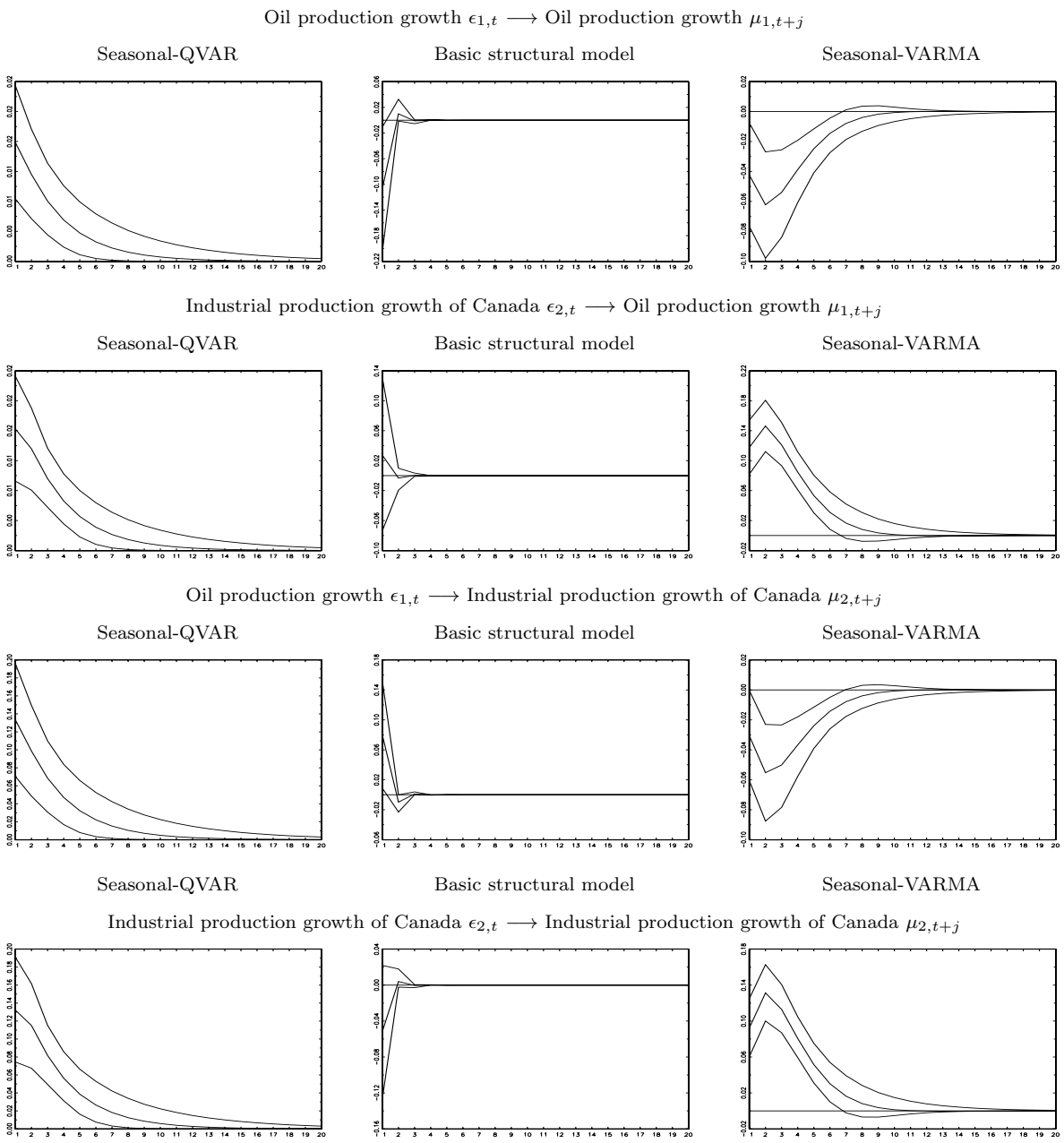

Fig. 14. Impulse response function with 90% confidence interval for the variables: world crude oil production growth $y_{1,t}$ and total industrial production growth of Canada $y_{2,t}$ (Seasonal-QVAR; basic structural model; Seasonal-VARMA). The IRF confidence interval is estimated by using 10,000 Monte Carlo simulations from the ML estimates.

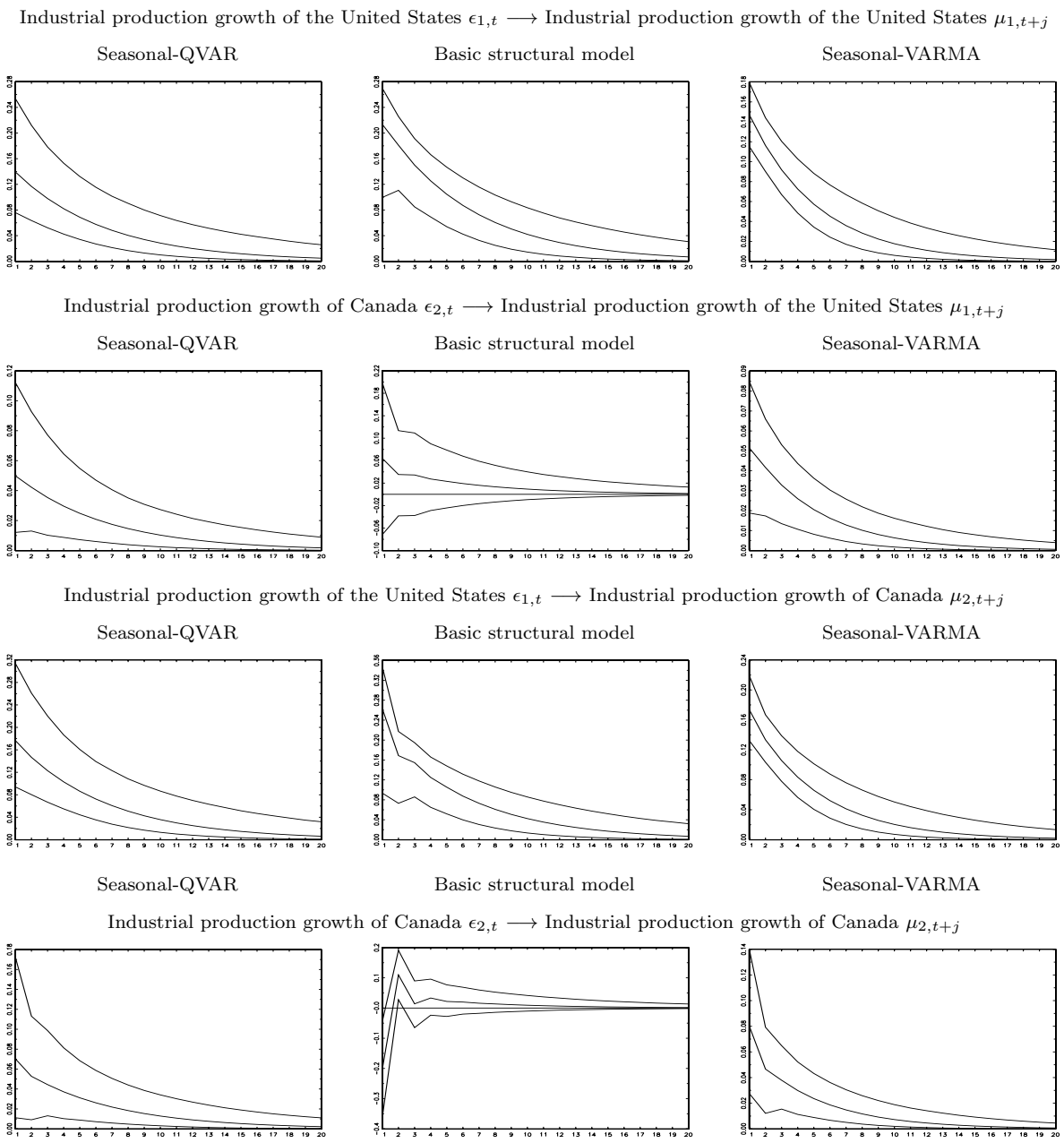

Fig. 15. Impulse response function with 90% confidence interval for the variables: total industrial production growth of the United States $y_{1,t}$ and total industrial production growth of Canada $y_{2,t}$ (Seasonal-QVAR; basic structural model; Seasonal-VARMA). The IRF confidence interval is estimated by using 10,000 Monte Carlo simulations from the ML estimates.

5. Conclusions

We have introduced the Seasonal-QVAR model with correlated seasonal and non-seasonal shocks. This new approach is an alternative to those recent UCM models, which use correlated seasonal and non-seasonal shocks. Seasonal-QVAR is also an alternative to the basic structural model and Seasonal-VARMA, which we have considered as benchmarks in our statistical analysis. We have applied Seasonal-QVAR to monthly macroeconomic time series data. We have used classic data from the variables: world crude oil production growth and global real economic activity growth for the period of March 1973 to December 2007. In addition, we have also used extended data from the variables: world crude oil production growth and total industrial production growths of the United States and Canada for the period of March 1973 to February 2018. The latter dataset has addressed an important applied economic question about the influence of world crude oil production on the industrial productions of the United States and Canada.

We have found that extreme observations in many cases appear in the irregular component of Seasonal-QVAR, while extreme observations for some cases appear in the local level component of the basic structural model and Seasonal-VARMA. We have found that the IRF estimates for the basic structural model are less precise than for Seasonal-QVAR. With respect to the interaction effects of the industrial production growth of the United States on world crude oil production growth, we have found that those effects are about six times higher for the basic structural model and Seasonal-VARMA than for Seasonal-QVAR. Our results suggest that the basic structural model and Seasonal-VARMA overestimate those effects. With respect to the interaction effects of world crude oil production growth on the industrial production growth of Canada, significant positive interaction effects have been found for Seasonal-QVAR, while significant negative interaction effects have been found for Seasonal-VARMA. Our results suggest that the interaction effects of world crude oil production growth on the industrial production growth of Canada are incorrectly estimated for Seasonal-VARMA. The results of the present paper may motivate the practical use of Seasonal-QVAR for the analysis of macroeconomic variables that involve significant seasonality components and extreme observations.

Acknowledgment

The work was presented in "Recent Advances in Econometrics: International Conference in Honor of Luc Bauwens" (Brussels, October 19-20, 2017), GESG Seminar (Guatemala City, December 7, 2017), "Workshop in Time Series Econometrics" (Zaragoza, April 12-13, 2018), and "International Conference on Statistical Methods for Big Data" (Madrid, July 7-8, 2018). The authors are thankful to Luc Bauwens, Matthew Copley, Antoni Espasa, Eric Ghysels, Joachim Grammig, Andrew Harvey, Søren Johansen, Bent Nielsen, Eric Renault, Genaro Sucarrat and Ruey Tsay. Blazsek and Licht acknowledge funding from Universidad Francisco Marroquín. Escribano acknowledges funding from Ministry of Economics, Spain (ECO2016-00105-001, MDM 2014-0431) and Community of Madrid (MadEco-CM S2015/HUM-3444).

Appendix. Seasonality component in DCS models

Each element of the seasonality component is modeled as:

$$s_{k,t} = D_t' \rho_{k,t} = D_{1,t}\rho_{k,1,t} + D_{2,t}\rho_{k,2,t} + \ldots + D_{S,t}\rho_{k,S,t} \tag{A.1}$$

The vector of dynamic seasonal parameters is $\rho_{k,1}$ for $t = 1$ and $\rho_{k,t} = \rho_{k,t-1} + \gamma_{k,t}u_{k,t-1}$ for $t = 2, \ldots, T$. By recursive substitution, we obtain that $\rho_{k,t} = \rho_{k,1} + \gamma_{k,2}u_{k,1} + \ldots + \gamma_{k,t}u_{k,t-1}$, where $\rho_{k,1}$ is the vector of initial values of $\rho_{k,t}$. Then, each element of $\rho_{k,t}$ is given by

$$\rho_{k,j,t} = \rho_{k,j,1} + \gamma_{k,j,2}u_{k,1} + \ldots + \gamma_{k,j,t}u_{k,t-1} \tag{A.2}$$

for $j = 1, \ldots, S$. Substituting Equation (A.2) into Equation (A.1) we get:

$$\begin{aligned} s_{k,t} &= D_{1,t}(\rho_{k,1,1} + \gamma_{k,1,2}u_{k,1} + \ldots + \gamma_{k,1,t}u_{k,t-1}) + \\ &+ D_{2,t}(\rho_{k,2,1} + \gamma_{k,2,2}u_{k,1} + \ldots + \gamma_{k,2,t}u_{k,t-1}) + \\ &+ D_{3,t}(\rho_{k,3,1} + \gamma_{k,3,2}u_{k,1} + \ldots + \gamma_{k,3,t}u_{k,t-1}) + \\ &+ \vdots \\ &+ D_{S,t}(\rho_{k,S,1} + \gamma_{k,S,2}u_{k,1} + \ldots + \gamma_{k,S,t}u_{k,t-1}) \end{aligned} \tag{A.3}$$

In Equation (A.3), the dummy variables select each one of the terms consecutively for each t. The selected value of $s_{k,t}$ is zero on average for consecutive $j = 1, \ldots, S$ time periods, because the average of each term within the parentheses of Equation (A.3) is zero. To see this, consider first the NLS procedure used for the estimation of the initial values of $\rho_{k,t}$, which ensures that $\rho_{k,1,1} + \rho_{k,2,1} + \ldots + \rho_{k,S,1} = 0$. Thus, $(\rho_{k,1,1} + \rho_{k,2,1} + \ldots + \rho_{k,S,1})/S = 0$. In addition, for all terms where $\gamma_{k,j,t}$ appears, $\gamma_{k,1,t} + \gamma_{k,2,t} + \ldots + \gamma_{k,S,t} = 0$, because for $j = 1, \ldots, S$, we parameterize $\gamma_{k,j,t} = \gamma_{k,j}$ for $D_{j,t} = 1$ and $\gamma_{k,j,t} = -\gamma_{k,j}/(S-1)$ for $D_{j,t} = 0$. Thus, $(\gamma_{k,1,t}u_{k,t-1} + \gamma_{k,2,t}u_{k,t-1} + \ldots + \gamma_{k,S,t}u_{k,t-1})/S = 0$. Therefore, the average of $s_{k,t}$ is also zero.

References

Ayala, A. and S. Blazsek (2017). New score-driven models for trimming and Winsorizing: an application for Guatemalan Quetzal to US Dollar. GESG Discussion Paper 2/2017, Universidad Francisco Marroquín.

Ayala, A. and S. Blazsek (2018). Score-driven models of local level, seasonality and volatility: an application to the currency exchange rate of Indian rupee to USD. GESG Discussion Paper 1/2018, Universidad Francisco Marroquín.

Ayala, A., S. Blazsek, and A. Escribano (2017). Dynamic conditional score models with time-varying location, scale and shape parameters. Working Paper 17-08, Carlos III University of Madrid, Department of Economics.

Barsky, R. B. and L. Kilian (2002). Do we really know that oil caused the Great Stagflation? A monetary alternative (pp. 137–183). In: B. S. Bernanke and K. Rogoff, eds., *NBER Macroeconomics Annual 2001* (Cambridge: MIT Press).

Barsky, R. B. and L. Kilian (2004). Oil and the macroeconomy since the 1970s. *Journal of Economic Perspectives 18*(4), 115–134.

Baumeister, C. and G. Peersman (2013). Time-varying effects of oil supply shocks on the US economy. *American Economic Journal: Macroeconomics 5*(4), 1–28.

Baumeister, C. J. S. and J. D. Hamilton (2017). Structural interpretation of vector autoregressions with incomplete identification: revisiting the role of oil supply and demand shocks. NBER Working Paper, no. 24167.

Baxter, M. and R. G. King (1999). Measuring business cycles: approximate band-pass filter for economic time series. *The Review of Economics and Statistics 81*(4), 575–593.

Bernanke, B. (1986). Alternative explorations of the money-income correlation. *Carnegie-Rochester Conference Series on Public Policy* (Amsterdam: North-Holland Publishing, 1986).

Blanchard, O. J. (2002). Comments on 'Do we really know that oil caused the Great Stagnation? A monetary alternative' by Robert Barsky and Lutz Kilian (pp. 183–192). In: B. Bernanke and K. Rogoff, eds., *NBER Macroeconomics Annual* (Cambridge: MIT Press).

Blanchard, O. and M. W. Watson (1986). Are all business cycles alike? In: R. J. Gordon, ed., *The American Business Cycle* (Chicago: Chicago University Press).

Blasques, F., P. Gorgi, S. J. Koopman, and O. Wintenberger (2018). Feasible invertibility conditions and maximum likelihood estimation for observation-driven models. *Electronic Journal of Statistics 12*(1), 1019–1052.

Blazsek, S. and A. Escribano (2016). Score-driven dynamic patent count panel data models. *Economics Letters 149*, 116–119.

Blazsek, S., A. Escribano, and A. Licht (2017). Score-driven nonlinear multivariate dynamic location models. Working Paper 17-14, Universidad Carlos III de Madrid, Department of Economics.

Blazsek, S. and H. Hernández (2017). Analysis of electricity prices for Central American countries using dynamic conditional score models. *Empirical Economics*, 1–42. doi: 10.1007/s00181-017-1341-3.

Blundell, R., R. Griffith, and F. Windmeijer (2002). Individual effects and dynamic in count data models. *Journal of Econometrics 108*(1), 113–131.

Bollerslev, T. (1986). Generalized autoregressive conditional heteroskedasticity. *Journal of Econometrics 31*(3), 307–327.

Box, G. E. P. and G. M. Jenkins (1970). *Time Series Analysis, Forecasting and Control.* (San Francisco: Holden-Day).

Caivano, M., A. C. Harvey, and A. Luati (2016). Robust time series models with trend and seasonal components. *SERIEs Journal of the Spanish Economic Association 7*(1), 99–120.

Cox, D. R. (1981). Statistical analysis of time series: some recent developments. *Scandinavian Journal of Statistics 8*(2), 93–115.

Creal, D., S. J. Koopman, and A. Lucas (2013). Generalized autoregressive score models with applications. *Journal of Applied Econometrics 28*(5), 777–795.

Davidson, R. and J. G. MacKinnon (2003). *Econometric Theory and Methods.* (New York: Oxford University Press).

Dickey, D. A. and W. A. Fuller (1979). Distribution of the estimators for autoregressive time series with a unit root. *Journal of the American Statistical Association 74*(366), 427–431.

Engle, R. F. (1982). Autoregressive conditional heteroscedasticity with estimates of the variance of United Kingdom inflation. *Econometrica 50*(4), 987–1007.

Escanciano, J. C. and I. N. Lobato (2009). An automatic Portmanteau test for serial correlation. *Journal of Econometrics 151*(2), 140–149.

Gouriéroux, C., A. Monfort, and A. Trognon (1984). Pseudo maximum likelihood methods: theory. *Econometrica 52*(3), 681–700.

Hamilton, J. D. (1994). *Time Series Analysis.* (Princeton: Princeton University Press).

Hamilton, J. D. (2003). What is an oil shock? *Journal of Econometrics 113*(2), 363-398.

Harvey, A. C. (1989). *Forecasting, Structural Time Series Models and the Kalman Filter.* (Cambridge: Cambridge University Press).

Harvey, A. C. (2013). *Dynamic Models for Volatility and Heavy Tails.* (Cambridge: Cambridge University Press).

Harvey, A. C. and T. Chakravarty (2008). Beta-t-(E)GARCH. Cambridge Working Papers in Economics 0840, Faculty of Economics, University of Cambridge.

Harvey, A. C. and A. Luati (2014). Filtering with heavy tails. *Journal of the American Statistical Association 109*(507), 1112–1122.

Hindrayanto, I., J. P. A. M. Jacobs, D. R. Osborn, and J. Tian (2018). Trend-cycle-seasonal interactions: identification and estimation. *Macroeconomic Dynamics*, 1–26. doi: 10.1017/S1365100517001092.

Kalman, R. E. (1960). A new approach to linear filtering and prediction problems. *Journal of Basic Engineering 82*, 35–45.

Kilian, L. (2008). A comparison of the effects of exogenous oil supply shocks on output and inflation in the G7 countries. *Journal of the European Economic Association 6*(1), 78–121.

Kilian, L. (2009). Not all oil price shocks are alike: disentangling demand and supply shocks in the crude oil market. *American Economic Review 99*(3), 1053–1069.

Kilian, L. and H. Lütkepohl (2017). *Structural Vector Autoregressive Analysis.* (Cambridge: Cambridge University Press).

Lütkepohl, H. (2005). *New Introduction to Multivariate Time Series Analysis.* (Berlin Heidelberg: Springer-Verlag).

Newey, K. and K. D. West (1987). A simple, positive semi-definite, heteroskedasticity and autocorrelation consistent covariance matrix. *Econometrica 55*(3), 703–708.

Nordhaus, W. D., H. S. Houthakker, and J. D. Sachs (1980). Oil and economic performance in industrial countries. *Brookings Papers on Economic Activity 2*, 341–399.

Peersman, G. and I. Van Robays (2009). Oil and the Euro Area Economy. *Economic Policy 24*(60), 603–651.

Raunglerdpanyagul, W. (1985). The seasonal pattern of shipping freight rates. Theses and Major Papers, Paper 298, University of Rhode Island.

Sims, C. A. (1980). Macroeconomics and reality. *Econometrica 48*(1), 1–48.

Sims, C. A. (1986). Are forecasting models usable for policy analysis? *Quarterly Review Federal Reserve Bank of Minneapolis 10*(1), 2–16.

Sims, C. A., S. M. Goldfeld, and J. D. Sachs (1982). Analysis with econometric models. *Brookings Papers on Economic Activity 1*, 107–164.

Stock, J. H. and M. W. Watson (2001). Vector autoregressions. *Journal of Economic Perspectives 15*(4), 101–115.

Tiao, G. C. and R. S. Tsay (1989). Model specification in multivariate time series. *Journal of the Royal Statistical Society 51*(Series B), 157–213.

Wooldridge, J. M. (2005). Simple solutions to the initial conditions problem in dynamic, nonlinear panel data models with unobserved heterogeneity. *Journal of Applied Econometrics 20*(1), 39–54.

Ye, M., J. Zyren, and J. Shore (2006). Forecasting short-run crude oil price using high- and low-inventory variables. *Energy Policy 34*, 2736–2743.